

A. a. XI.

REPORT No. 222
GEOLOGICAL SURVEY OF JAPAN

**FRACTURE SYSTEM OF OSHIMA ISLAND,
KYUSHU : A STUDY OF JOINTING IN
BRITTLE SEDIMENTARY ROCKS**

By

Kazuo HOSHINO

GEOLOGICAL SURVEY OF JAPAN

Hisamoto-chō, Kawasaki-shi, Japan

1967

Corrigenda

Kazuo HOSHINO : Fracture System of Oshima Island, Kyushu
Report, Geological Survey of Japan, No. 222, 1967

page	line	read	for
1	(Abstract) 4	Group A includes	A group include
//	// 6	Group A is	A group are
//	// 6	while B group is	while B group are
//	// 7	C group contains	C group contain
//	// 8	D group consists of	D group consist of
//	// 9	reverse faults of low angle	reverse faults with low angle
//	// 11	Among the groups, B-1 is	Among the groups, B-1 are
//	// 11	and contains the most	and contain the most
//	// 13	B-1 group is found	B-1 group are found
//	// 17	In most places B-1 is found	In most places B-1 are found
//	// 28	the old Yobuko Strait fault	the Yobuko Strait fault
10	14	that tectonically important	that kinds of
14	24	A-2 group was	A-2 group were
22	Table 3	fracture set	fracture set
		B1a	B1a
		B1a	a
		B1b	b
		B1a	a
		B1a	a
		B1a	a
		B1a	a
		B1a	a
		B1a	a
24	21	group of low dip is probably	group of low dip are probably
26	*foot notes	the direct connection of the two faults was observed	the direct connection of the two faults were observed
27	Explanation of Fig. 24	Right : C group is	Right : C group are
29	2	in Higure	in Higure
29	5	C group was resulted	C group were resulted
30	5	A-1 group is	A-1 groups are
//	22	C group is	C group are
31	1	C group is considered	C group are considered
35	1	B-2 group develops	B-2 group develop
37	29	$\phi = \frac{a}{6}x^3 + \frac{b}{2}x^2y + \frac{c}{2}xy^2 +$	$\phi = \frac{a_1}{6}x^3 + \frac{b_1}{2}x^2y + \frac{c_1}{2}xy^2 + \dots$
38	5	$\tau_{xy} = T$	$T_{xy} = -T$
//	11	$\tan 2z = \frac{2T}{(X-Y_1) - (Y_2-Y_1)\frac{x}{l}}$	$\tan 2z = \frac{-2T}{(X-Y_1) - (Y_2-Y_1)\frac{x}{l}}$
//	12	no printed	$\tan 2z = \frac{-2T}{(X-Y_1) - (Y_2-Y_1)\frac{x}{l}}$

page	line	read	for
38	24	$z = q$, when $x = l$, or $m = 1$	$z = q$, when $x = l$, or $m = l$
//	27	$p = -18^\circ$, and $q = -12^\circ$	$p = 18$, $q = -12$
//	29	$ \sigma_m \geq \sigma \sin \varphi + \dots$	$\sigma_m^2 \geq \sigma \sin \varphi + \dots$
//	32	$\sigma_m = \frac{1}{2}(\sigma_1 - \sigma_3) =$	$\sigma_m \frac{1}{2}(\sigma_1 - \sigma_3) =$
39	10	$Y_1 < -\frac{1}{2} \left(\frac{P}{\sin \varphi} + Q \right)$	$Y_1 < \frac{1}{2} \left(\frac{P}{\sin \varphi} + Q \right)$
//	14	kg/cm ² ,	kg/cm ²
//	18	Y_1 is negative	Y is negative
//	19	For $(Y_2 - Y_1) < -460 \text{ kg/cm}^2$, Y_1 can be	For $(Y_2 - Y_1) > -460 \text{ kg/cm}$, Y_1 is
42	13	contrast, if being $(Y_2 - Y_1) > 0$,	contrast, being $(Y_2 - Y_1) > 0$,
44	12	B-2 group is	B-2 group are
45	30	the places where the angle	the places that the angle
//	30	getting zero is where	getting zero is that
47	28	Most of B-1 are found	Most of B-1 is found
49	13	From line 13, a separate paragraph	
50	24	B-2 are faults that are	B-2 are faults which are
//	25	that of B group is	that of B sets are
//	35	B-2 group is formed	B-2 group are formed
//	43	as the beginning of the initial fracturing.	as the initial fracturing begin.



551.24 : 553.94 (522, 2)

REPORT No. 222

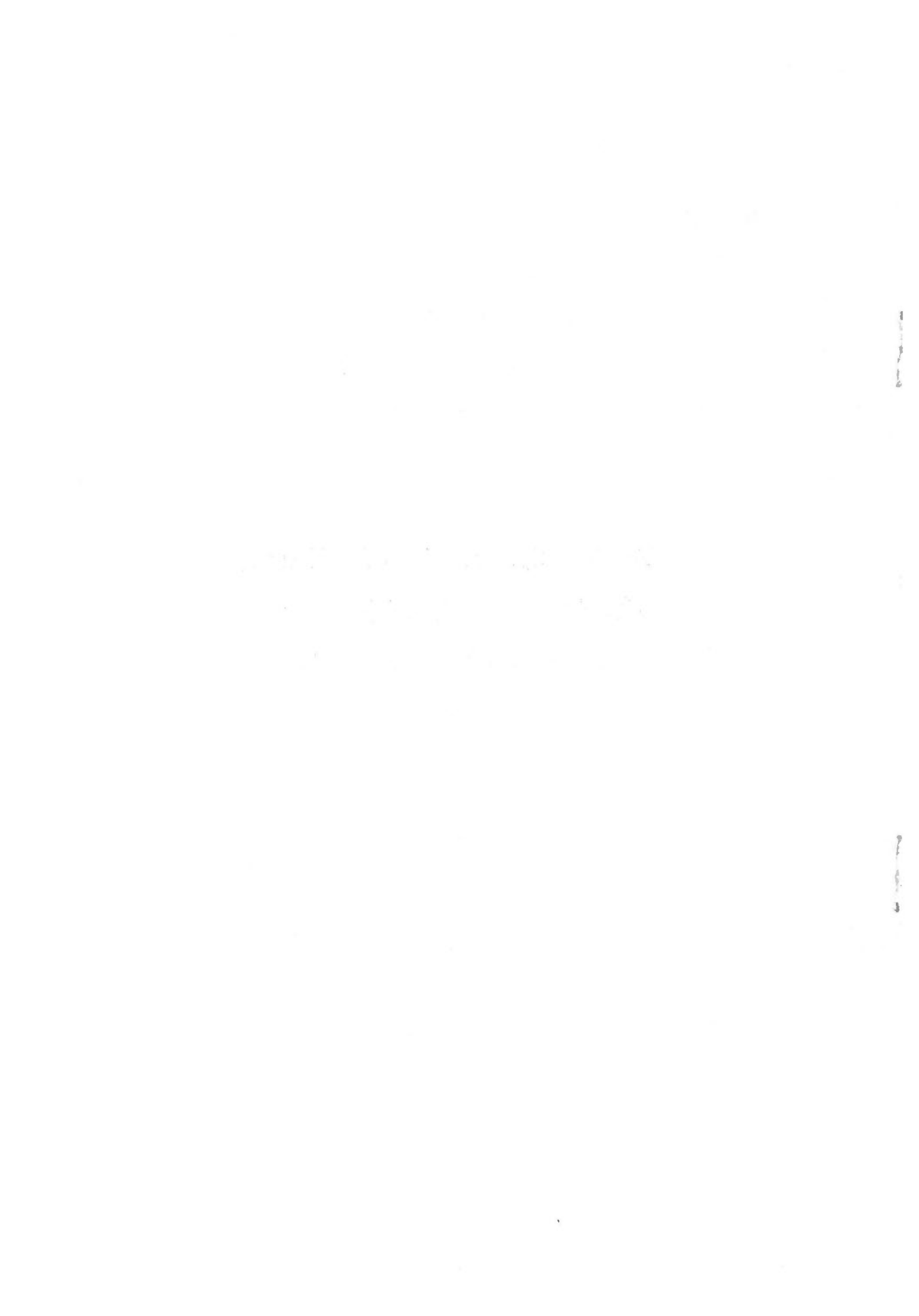
GEOLOGICAL SURVEY OF JAPAN

Konosuke SATO, Director

Fracture System of Oshima Island,
Kyushu : A Study of Jointing in
Brittle Sedimentary Rocks

By

KAZUO HOSHINO



CONTENTS

	Page
Abstract	1
I. Introduction	1
II. General Geology	5
II. 1 Location and topography	5
II. 2 Stratigraphy	5
II. 3 Geological structure	7
II. 4 Faults	8
III. Method of Fracture Study and Definition	9
IV. Description of the Fracture Groups	13
IV. 1 A group	13
IV. 1. 1 A-1 group	13
IV. 1. 2 A-2 group	14
IV. 1. 3 A-3 group	15
IV. 2 B group	19
IV. 2. 1 B-1 group	19
IV. 2. 2 B-2 group	26
IV. 3 Other fracture groups	28
IV. 3. 1 C group	28
IV. 3. 2 D group	29
V. Age of Fracturing and the Change of Stress Field	30
V. 1 Age of the fracture group	30
V. 2 The stress fields at the fracturings during III and IV periods	32
V. 3 The Yobuko Strait faults and the tectonic history in Oshima area	34
VI. The Boundary Stresses at the Fracturing of B-1 Group	36
VI. 1 Introduction	36
VI. 2 Calculation upon the assumption of elastic and brittle deformation	37
VI. 3 Geological implication of the result of calculation	40
VII. Jointing and Faulted Zones	43
VII. 1 The angle of shear	43
VII. 2 Extension and shear fractures	45
VII. 3 Faulted zones	45
VIII. Mechanism of the Jointing in Ōshima Area	47
IX. Conclusion	50
Appendix	51
References	53
要 旨	
Plates 1 ~ 6	

Fracture System of Oshima Island, Kyushu : A Study of Jointing in Brittle Sedimentary Rocks

By
Kazuo HOSHINO*

Abstract

Because of long shoreline with abundant places of topographic complexity, Ōshima, a tiny island in northwestern Kyushu is a good place for obtaining a complete fracture pattern in a whole area. Four fracture groups were distinguished on basis of parallelism, mode of displacement and age. A group include 3 groups and are approximately north to southward in strike. B group includes 2 and are approximately east to westward in strike. A group are the most predominant fracture group in Terashima, while B group are the most predominant in Ōshima and Ōtawa. C group contain the fracture that is vertical to the bedding planes and parallel either to the strike or dip. D group consist of small reverse faults with low angle that have various strike and dip. The mode of occurrence and characteristics of the fracture group are given in Table 6.

Among the groups, B-1 are most frequent and contain the most systematic Joints. B-1a and B-1b make a conjugate set, the former being of left lateral and the latter of right lateral. The rocks in which B-1 group are found more conspicuous are Matsushima and Nishisonogi groups, which, consisting of sandstone and shale, about a thousand meter or less in thickness, exhibit a gentle structure isoclinally dipping westward at angle of less than 10° . They are very hard and brittle up to 1,000 or 1,500 bars of confining pressure.

In most places B-1 are found as joints in good parallelism, however they are faulted at rather constant interval of 1 km. It is rarely found at outcrops that B-1a and B-1b intersect each other. Around the place of possible intersection, there are extension fractures, B-1c in most cases.

At 98 localities, principal stresses of B-1 were found, (Fig. 11). Maximum principal stress lines are rather simple curve concaved slightly to the south. With this curve as a model shown in Fig. 32, boundary stresses were calculated by using Airy function under the presumption that the rocks made brittle deformation and were fractured by Mohr's criterion. The result indicates that the boundary stress along minimum principal stress, trending approximately north to south is tensile stress. Geological interpretation also suggests that the fracturing of B group as well as A group was resulted from upward movements which possibly occurred at least twice after Nishisonogi along the Yobuko Strait fault.

It is concluded that the joint is the fracture that has little displacement along the planes and that would be formed in brittle rocks when the rocks fail in low stress field such as tensile stress.

I. Introduction

Fracture pattern has been an important subject in structural geology. In most places, fracture system has been found to be geometrically systematic over wide area and to have

* Fuel Department

genetical relation to the structural features. Joints, among various kinds of fracture, has been most studied because of their characteristic appearance and abundant existence. Joints are generally defined as the fractures that along the planes there is no cohesion and no visible shift, (HODGSON, 1961 a). Besides, "Joints" should not be alone, but should accompany some parallel planes as suggested etymologically from term "to join" joints, (BILLINGS, 1954). Foliation is also the fracture that is classified on the basis of parallelism. However, foliation is related to metamorphic rocks and the sedimentary rocks of old age, while joints are referred to younger rocks.

Field study of joints and joint pattern have been done for many years. WAGER (1931) found that the joints in the limestone near Craven exhibit constant trends in large area, and concluded that the joints might have been formed by shear stress. WAGER consulted some experimental results by BUCHER (1920, 1921) to make his conclusion. SHELDON (1912), PARKER (1942), VER STEEG (1942), NICKELSEN and HOUGH (1958) studied the jointing in Allegheny Plateau in northwestern United States. SPENCER (1959), HODGSON (1961 a. b.), WISE (1964) studied the fracture system of the basement rocks in Montana and Wyoming. HARRIS and others (1960), MELTON (1929), and KELLEY and CLINTON (1960) published work on joints in various places. In Japan, there have been many workers who studied joints in sedimentary rocks from various standpoints. They are MURAI (1952, 1955, 1965, 1966), KITAMURA (1962), and KIMURA (1966). With these contributions, a lot of field data that might indicate geological and physical environments favoring the formation of joints have been piled up, however, we have not a satisfactory theory of jointing yet.

Little movement along the joint-planes indicates that joints are an extension fracture. Often we find feathers-like structure named plumose structure on some joint planes. HODGSON (1961 a, b) interpreted plumose structure as an indication of extension origin of the joints. However, if extension origin is admitted, it is difficult to explain "oblique joints", (DE SITTER, 1956; PEICE, 1959). Many workers (DE SITTER, 1956; HOSHINO, 1963; PARKER, 1942; SPENCER, 1959) reported a possible existence of the pair which consists of two joint sets making a constant acute angle of 40° to 60° over a large area. In many cases, the bisector of the acute angle of the pair is closely related to the folding axes and the trends of faults. These observations strongly indicate that joints are not always extension fracture. Some joints should be classified as shear fracture even if they have no visible movement along the planes.

Then, is it possible to do theoretical explanation how shear fracture can be occurred in rather wide extent as of non-movement fracture like joints? For these 10 years, experimental work under high confining pressure have made a remarkable progress. GRIGGS, HANDIN, HEARD, ROBERTSON, DONATH and BRACE have done the experimentation to find out the condition and the mechanism of fracturing. The work by PATTERSON (1958), GRIGGS and HANDIN (1960) and DONATH (1964) made it clear that as mode of deformation changes brittle to ductile, fracture does from extension fracture, single shear to net-work shear fracture and finally in very ductile to flow, without any exception. To indicate the degree of transition from brittle to ductile, GRIGGS and HANDIN defined strain % at fracturing as ductility, (refer HOSHINO, 1966). Ductility is a function of rock material, confining pressure, temperature and so on. Among them, confining pressure is most important factor. Generally, it is indicated that as confining pressure increases, ductility increases. MOGI (1964, 1965) did a series of high pressure test on Japanese rocks. According to his results, the above description is supported, too.

Previous work clearly indicates that the joints are found best in such rocks as

- (1) the rocks being nearly horizontal, influenced by little tectonic movement.
- (2) the greatest depth that the rocks have had is not so large, but the rocks was buried to enough depth and elapsed enough time to complete cementation.
- (3) compact or massive hard rocks.

The more the rocks exhibit such a character, the more apparently little-shift, and parallelism of the joints is expressed. The more the condition (1) is satisfied in the rocks, the better the regional joints, which are the fracture that keeps consistency in trend over a large area, (PRICE, 1959) are formed.

Condition (2) and (3) indicate that joints are result of brittle deformation. Hard, compact rocks are brittle even in considerable large confining pressure. Shallow depth indicates small confining pressure, so shallow depth is a good condition for brittle deformation. In brittle deformation, rocks fail at low strain (possible less than 2 or 3%). Even if all this strain is released as the movement along the fracture planes, it is probable that the movement along each plane is extremely little because of high density of fracturing in brittle deformation.

Condition (1) indicates the environment of low tectonic stress such as of tensile stress. PRICE (1959) described that the tensile stress resulted from uplift movement of the crust might be responsible for jointing. MUELBERGER (1961) made a good use of Leon-Mohr criterion of failure to explain the mechanism of the conjugate set of joints which he observed to be shear fracture having small dihedral angle. According to Leon-Mohr criterion, the angle of shear fracture is getting smaller in low confining stress. The critical point that the angle equals to zero, the fracture should be called extension fracture substantially. MUELBERGER (1961) interpreted that what the joint in Allegheny Plateau studied by PARKER (1942) have both characters of shear and extension fracture - it has angle of shear of approximately 19° as well as it has plumose structure, is quite reasonable if we apply Leon-Mohr criterion for this case. SECOR (1965), upon the basis of the presumption that there is no genetical relation between the joint system and structural features, thought the joints as an extension fracture. However, at the same time he admitted that some joints can be shear fracture in high stress field such as in a deep place and in the place influenced by much deformation. BRACE (1964) described that complete transition is suggested between extension and shear fractures.

In these ways, it seems that the worker's thinkings upon the mechanism of the jointing is coming to an agreement to some degree. However, still there have been lack of field data which could be basis to these thinkings.

Difficulties of the field study of joints exist mostly in little displacement of the joint planes. In order to solve such questions, it is necessary to classify fracture sets, to decide time relation among them and to know mode of displacement of the fracture. Because of the little displacement, in joints, it would be difficult to know either time relation or mode of displacement. The author have studied the fracture system in Japanese coal and oil fields for several years (HOSHINO, 1962, 1963, 1965). In all places, he met such difficulties. Concerning this point, Ōshima, a tiny island in northwestern Kyushu is a very good place for joint study. It has an indented shoreline and at low tide we can walk continuously from place to place to trace every place of outcrop on the shore. A lot of drifts for coal seams in the depth of 700m at most make it possible to know vertical change of the fracture pattern as well as the horizontal change below the surface. In Ōshima, it was possible to know structural relation between the joints and the faults, and exact pattern of joints and mutual relation among the fracture sets better than any other places.

Chapters 2, 3 and 4 contain explanation about general geology and the method of

study and description of the result of field study.

In chapter 5, some considerations about the age of the fracture group and the change of principal stresses will be made on the basis of previous geological work and the result of field study. Chapters 6, 7 and 8 are the discussion about the mechanism of jointing in Ōshima area. The discussion was made mostly of B-1 set which contains a lot of dense parallel joints and is most conspicuous fracture sets in this area. In chapters 6, 7 and 8, therefore, field data that would indicate the environment and mechanism of the fracturing such as degree of stress at fracturing, the relation between extension and shear joints and the condition of fracturing is studied quantitatively as well as possible.

What should be done for better understanding of the cause and mechanism of jointing would be to make geological and physical condition at the jointing clear in many fields. It would be premature to think that the condition found good at a field is applicable to other fields. Most important thing for the study of joints at the present would be to begin with case studies of various places.

Acknowledgements

The author thanks Prof. Toshio KIMURA for valuable comment and critical reading of the manuscript. He wishes to thank Prof. Shōzaburo NAGUMO, Prof. Fuyuji TAKAI, Prof. Kozō KAWAI, Prof. Takeo WATANABE, Prof. Tadashi SATŌ, Dr. Kinji TSURUTA, Dr. Yasufumi ISHIWADA, Dr. Shingorō IJIMA for helpful discussion and kind encouragement. Thanks are also due to Mr. H. ENDŌ, Mr. YAGI and other personnel of the Ōshima

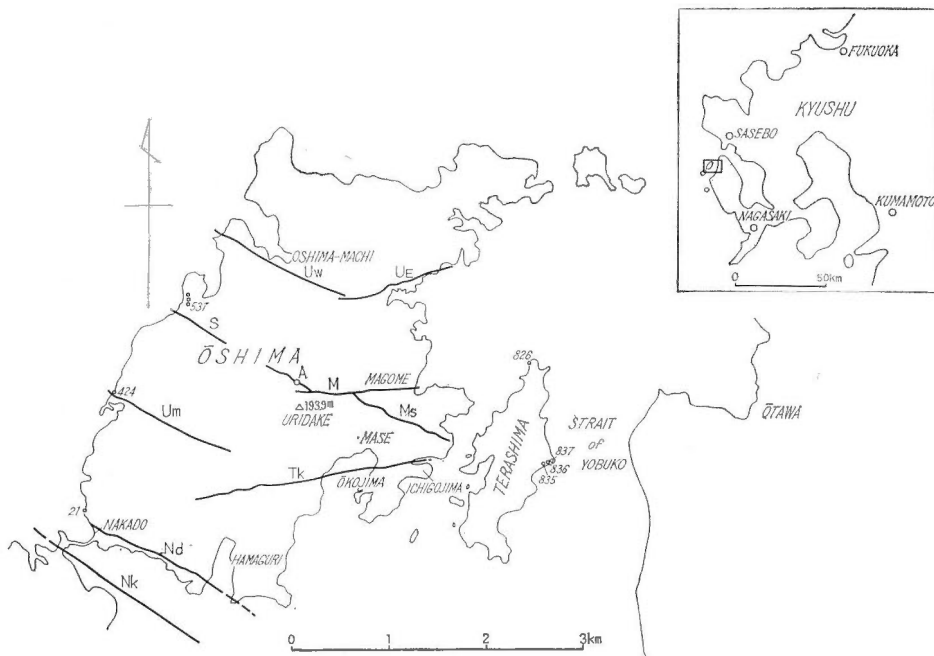


Fig. 1 Locality and index map

Mining Branch, Matsushima Coal Mining Co., for kind help and hospitality during the author's field study in Ōshima. The author is also indebted to Mr. Shuntarō FURUKAWA and Kiyoto KIYOHARA for their helps during the field mapping in Ōshima.

II. General Geology

II. 1 Location and topography

Ōshima is a small island, 15 km southwest from Sasebo city, 5 km × 14 km in area and 29 km in the length of the shoreline. Terashima, located a little east of Ōshima is a slender island, and 1 km × 5 km in area. Eastward from Terashima, there is Yobuko Strait, approximately 2 km in width and if going eastward more, there is Ōtawa town in Nishisonogi Peninsula, a part of Kyushu mainland, (Fig. 1).

Both Ōshima and Terashima exhibit questa structure that is composed of approximately 10° to 30° westward dipping strata. The highest place in Ōshima is the top of Uridake, and 193.3 m high above the sea level.

Table 1

Age	Group	Formation	Rocks	Thickness. (m.)
	<i>Basalts</i>			
Mid. or Late Oligocene	Nishisonogi (Kishima)	Higire	alt; ss, sh	90
		Shioda	c ss,	50
		Yuridake	alt; sh, ss c-m ss	110
		Tokuman	alt; sh, ss	55-110
		Mase	c ss	140-300
Earl. Oligocene	Matsushima g.		ss, ms, cg, coal.	5-200
Earl-Mid.	Terashima g.		ss, cg, ms	400
Eocene	Akazaki g.		ss, ms, cg	120
Pre- Tertiary	<i>Granites and Schists</i>			

II. 2 Stratigraphy

The oldest rocks are pre-Tertiary granite and mylonite, which are found in a restricted area in the eastern Terashima. Most part of the area consists of Paleogene sedimentary rocks. Terashima consists of Terashima and Akazaki groups, early and middle Eocene in age. These rocks are conglomerate and coarse sandstone. The thickness of Terashima is 400 m and that of Akazaki 120 m. In Ōshima, there are Matsushima group, early Oligocene in age and Nishisonogi group, middle and late Miocene. Matsushima group is a series of land deposit ranging 500 to 200 m in thickness. To northeastward and eastward it becomes thinner. Matsushima group covers Terashima with unconformity. In upper



Fig. 2 Geological map

part, it has several coal seams, thickness of which are 1 to 4 m. Some of them are being worked by Matsushima coal Mining Co.. Nishisonogi group occupies most part of Ōshima and it is marine sediments of coarse sandstone and alternation of sandstone and shale, approximately 600 m in thickness.

Above these sedimentary rocks, lava of basalt is found in the northern part of Oshima. This is probably same as that which is found in many places in northern Kyushu. It is dated, according to NAGAHAMA (1958), Pliocene to Pleistocene.

II. 3 Geological structure

General feature in Ōshima is an isoclinal structure dipping at approximately 10° westward. From west to east, therefore, there are found Akazaki, Terashima, Matsushima and Nishisonogi groups respectively.

The strike trends around $N 10 - 20^\circ E$. In southern Ōshima, the trend changes to $N 40^\circ W$, while in northern Ōshima to $E - W$, exhibiting something like dome structure around Terashima as shown in Fig. 3.

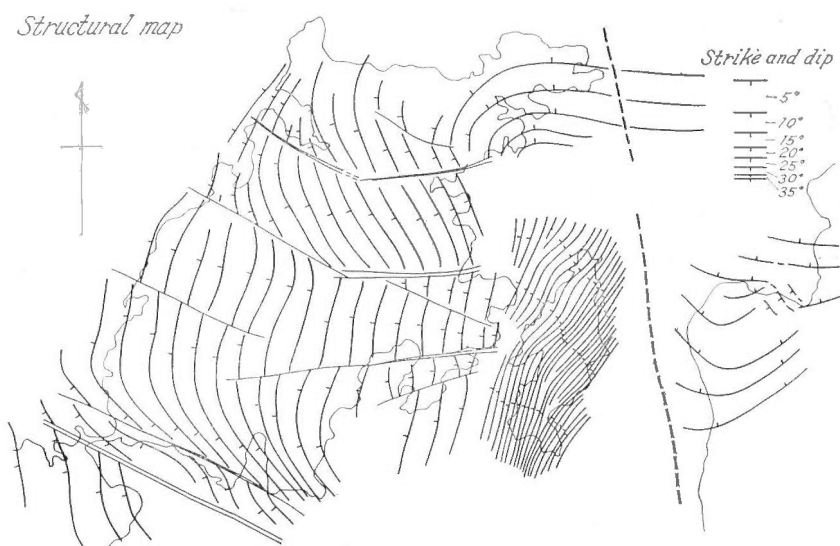


Fig. 3 Structural map

In Ōtawa and its neighbourhood, Akazaki, Terashima and Matsushima groups are not found. Horizontally dipping, Nishisonogi overlies directly upon pre-Tertiary crystalline schist. Mase formation, the lowermost in Nishisonogi is much thinner in Ōtawa than in Ōshima. However the strata above Uridake formation has almost same rock facies and thickness in both sides Ōshima and Ōtawa.

In eastern Terashima, dips are between 40° and 50° where Tertiary rocks cover the mylonite with unconformity. However, further to the west dips are getting to be nearly horizontal. In the western side of Ōshima, it ranges 8° to 6° at the surface or in upper Nishisonogi, and 6° to 0 in the drifts at the depth of several hundreds meters in coal

bearing Matsushima group. The structure in Kakinoura Island, southeast of Oshima indicates that a synclinal axis trending NNE or NE is to be found off the western coast of Oshima.

II. 4 Faults

As far as the observation on the rocks exposed at the surface concerned, there is much difference between the faults in Akazaki and Terashima and those in Matsushima and Nishisonogi groups. In Akazaki and Terashima groups, the faults trend N—S in average, approximately ranging from NNW—SSE to NNE—SSW. Most of them are small in displacement and length. On the other hand, in Matsushima and Nishisonogi groups, the faults trend E—W in average ranging from ENE—WSW to ESE—WNW. Some of them are quite large and apparent normal fault dipping northward. The E—W trending faults are found in Terashima although they are a few and small, and found to be formed later than N—S trending faults.

Table 2 Major faults

Abbreviation (refer. Fig. 1)	Name	Strike	Dip	Largest throw(m)	References
Ue	Kurose	N65°E		50	
Uw	Uchiura	N65°W		40	
S	Shioda	N70°W	65° N	20	hinge fault
Mg	Magome	E—W	45° N	220	dip slip
Tk	Tokuman	E—W	50° N	75	
Ms	Mase	N65°W	50° S	30	
Um	Umenoki	N70°W	50° N	10	
O	Okojima	N70°E		10	
Nk	Nakato	N65°W		20	
Nd	Noda	N70°W	65° N	65	strike slip

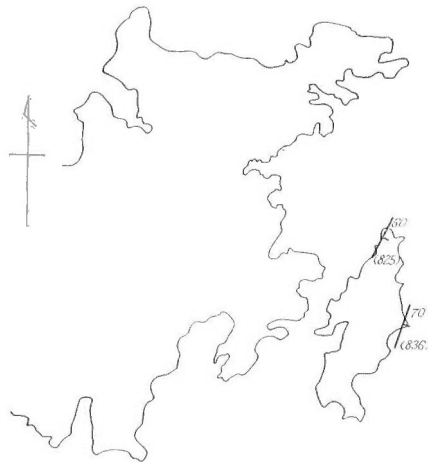


Fig. 4 Distribution of A-1 group

In Yobuko Strait, large faults named the Yobuko Strait faults were presumed by NAGAHAMA (1958, 1962) from the geological structure and stratigraphy in both sides. NAGAHAMA studied specially the faults from the points of the rock facies and the structure of Tertiary rocks. He thought that the faults had been active several times from pre-Tertiary period. The ages of main movements are

- 1) pre-Tertiary.
- 2) early Oligocene or between Terashima and Matsushima groups.
- 3) after Oligocene, or after Nishisonogi group.

His conclusion was confirmed by the author's field survey, except the last age. Fracture survey by the author indicated that the last movements are dated not to be one, but two periods of movements are expected to have existed after Nishisonogi, (refer 5.3). It will be described in latter pages, this last movements are related structurally not only to the Yobuko Strait faults and its parallel fractures but also to E—N fractures in Matsushima and Nishisonogi groups.

III. Method of Fracture Study and Definition

In this study, continuous observation of the rocks and the fractures was done very well because of long and complex shoreline and abundant clear cuts along roads.

Term *fractures* are used here as a general name for any plane which represents non-continuity or separation in the rocks. If displacement is seen along the planes with naked eye they are called *faults*. If no displacement is seen they are called *joints*. often we see irregular fractures that are formed with weathering or such artificial fractures as caused by dynamite blasting. Such fractures were excluded from the measurements this time.



Fig. 5 Distribution of A-2 group

Generally, it is difficult to classify on definite theoretical basis all fractures that are observed during field mapping. In this study, the classification was done by principle of

parallelism for the first. If, in outcrops considerable number of fractures are parallel with one another, these fractures are distinguished to make a **set**. Some planes of fractures of a set are measured on strikes and dips in a same way as bedding planes are measured, then a plane representing a set is known as the average plane among them. In this way, at each localities of the studied area the strikes and dips of sets were measured, and wrote down on a 1/5,000 route map in a same way as it is usually done of bedding planes, and as a result, **the fracture map** was completed. Here the measurements were done of the fractures more than one meter in apparent length only. During the field mapping, the mode of displacement, mutual relation in space and time, and magnitude of fractures were noted and sketched in the field notes.

The sets thus found are an expression of classification based upon observation. However, the fracture map could be said a general table which should include all fracture sets that are of importance in tectonic meaning and are related to structural development on regional scale more or less. In fact, it was indicated by the fracture map that kinds of fracture sets are comparatively a few and common through every locality of the studied area. Therefore, it would be possible for us to check the sets on regional scale with for time relation, characteristics of the fracture planes, mode of displacement, and so on, and to distinguish **group**. The fractures that are same in age and mode of displacement, and considered to be originated from tectonically same cause are mentioned as a group.

In same places, where the occurrence of fractures is too complicated to recognize sets, 100 fractures were measured at random method, plotted and contoured in the Schmidt net with statistical procedure and tentative poles of sets were decided.

As mentioned above, faults or joints were defined as whether the fractures are with or without visible displacement along the planes. Every facture was classified to either faults or joints according to this basis.

However, it seems there is no theoretical reason that we distinguish joints from faults. On the other hand, it happens very often that some faults are accompanied by the parallel joints and that, if we observe the rocks carefully, we see the change between both are undoubtedly transitional. This might suggest us that the both belong to the same genetical origin. **Fracture set** comprises **fault** and **joint sets**.



Fig. 6 Distribution of A-3 group

Upon experimental basis, fractures are classified as **extension** and **shear fractures**. Extension fractures are formed parallel to the plane that contains maximum and medium principal stresses, the displacement of which is parallel to minimum principal stress. Shear fractures are formed making an angle less than 45° to the plane that contains maximum and medium principal stresses. This angle is called **the angle of shear**, and written θ_s , or $2\theta_s$ here. In shear fractures, displacement occurs parallel to the fracture planes, in such a way that the rocks are apparently shortened by maximum principal stress. In brittle deformation, a **single shear fracture** is made, (PATTERSON, 1958), and so on. Being less brittle, two planes of shear fracture called **conjugate set of shear fracture** are made almost simultaneously being symmetrically on either sides of the plane that contains maximum and medium principal stresses. In transitional stage from brittle to ductile, considerable number of conjugate sets, the fractures of which are without visible displacement are formed in network-pattern (PATTERSON, 1958, MOGI, 1964, 1965, HOSHINO, 1966).

At the surface exposure where we found two sets of fractures, they are recognized as conjugate set, if they satisfied the next two conditions. (1) Both intersect or are expected to intersect [at the acute angle and the movement along the fracture planes would be in such way that should be done in conjugate set. (2) Both are formed simultaneously. If, (2) is not ascertained, and (1) only is satisfied, the two sets might be called conventionally **pair set (of shear fracture)**.

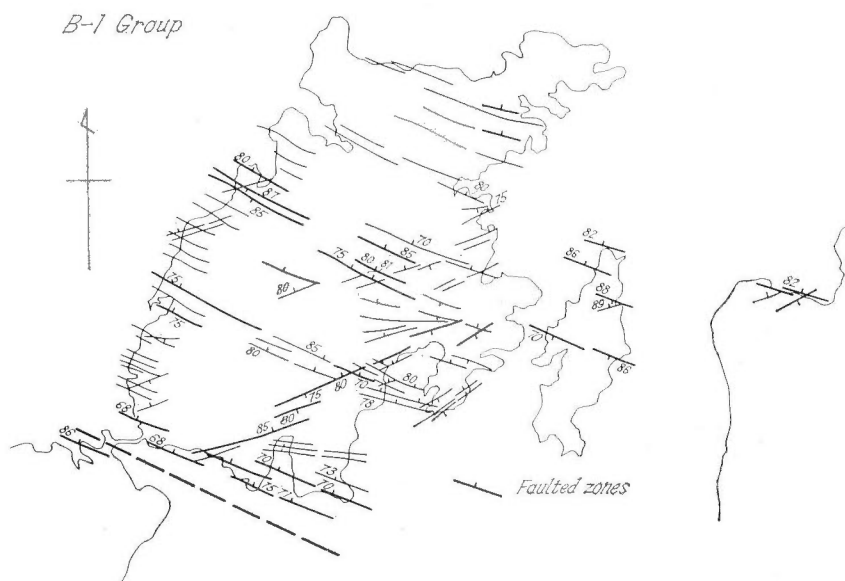


Fig. 7 Distribution of B-1 group

If any fracture is recognized to make conjugate set, we can decide the angle of shear and directions of principal stresses by going back the procedure mentioned above. $2\theta_s$ should be equal to the acute angle or the angle of shear. The bisector of the acute angle is the direction of maximum principal stress, the intersection of two single planes is the direction of medium principal stress and the minimum and medium principal stresses.

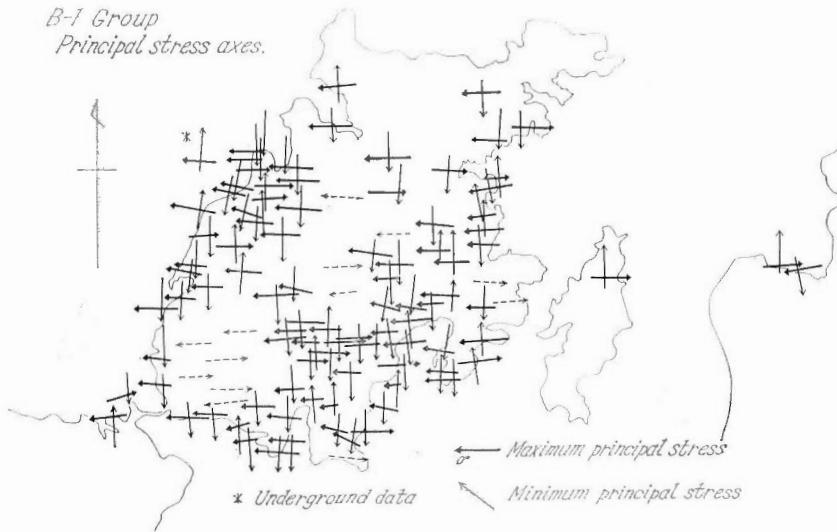


Fig. 8 Principal stresses at the fracturing of B-1 group

It was very difficult to distinguish extension fractures from shear fractures with observation of the fracture planes. In the fracture planes made by high pressure experimentation, it is often observed, extension fractures have curved irregular planes, while shear fractures have the traces of movement such as slicken side or surface structures caused by friction on the planes. The surface of shear fractures is plane in most cases.

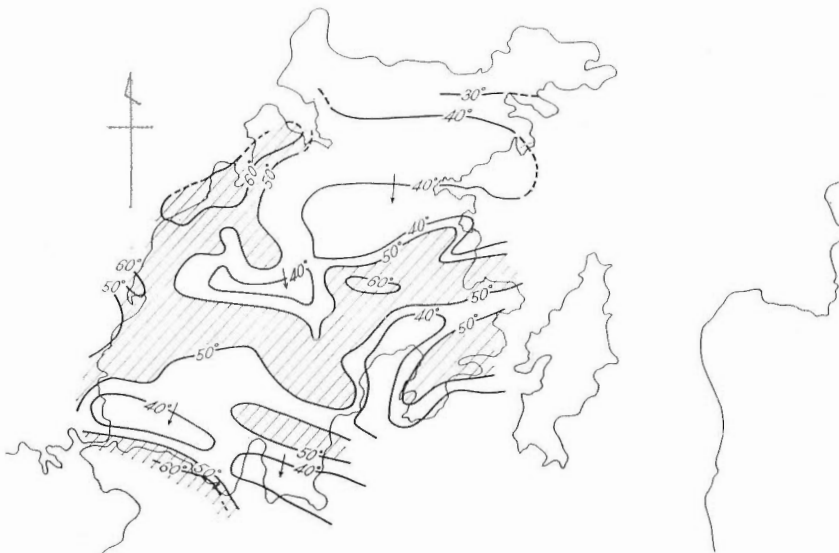


Fig. 9 Angle of shear fracture of B-1 group

lateral or reverse fault. It was found at two localities in Terashima, (Fig. 4). Locality 825 is found in Terashima group and Loc. 836 is in Akazaki group. Both localities are composed of conglomerate and alternation of conglomerate and sandstone, therefore it was easy to analyse mutual relation among fractures. A-1 group is clearly cut by A-2, A-3 and B group, and considered the oldest group. Most of A-1 group are found with visible displacement, which is small at most cases.

IV. 1. 2 A-2 group

The strike ranges between 10° and 50° W. A-2 group is divided into two groups; one, A-2a group which has average strike 40° W, dip 65° W and is apparently normal

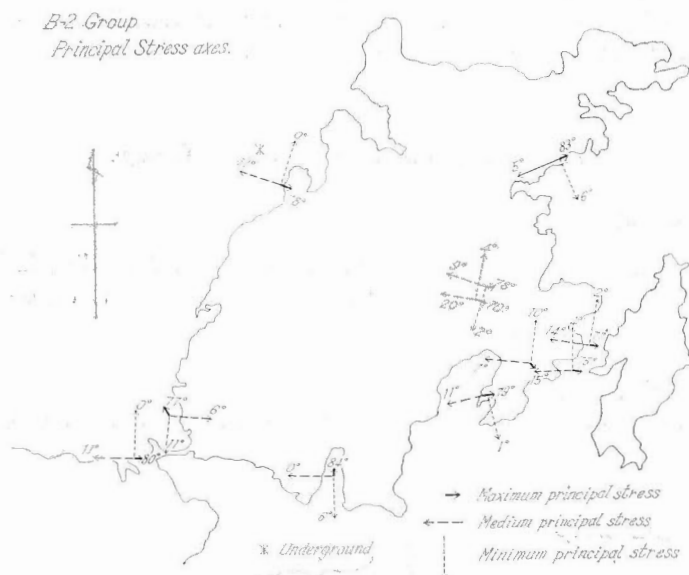


Fig. 11 Principal stresses at the fracturing of B-2 group

fault, the other, A-2a and A-2b make a conjugate set as shown in Fig. 15, A, C. If we decide maximum principal stress it is $N 38^\circ W, 88^\circ S$ and approximately equals to the pole of the bedding plane. The angle of shear $2\theta_s$ is 50° . If the poles of all A-2 fractures found in Terashima are plotted in a Schmidt net diagram, we see the poles are not clearly separated into two groups, one that should represent A-2a and the other that should represent A-2b, but the poles are distributed continuously and dispersedly between the two centres of concentration. With this figures, we might consider that what happened actually is something like that the angle of shear of individual set ranges between 0 and 90° , although statistically the angle is 50° . It is very interesting that in Fig. 16, the point of minimum principal stress comes on the middle line between poles of A-2a and A-2b. The area between the plotted line and the circle belongs to A-2b because the fractures in this area are of right lateral or apparently reverse faults, which suggest same nature as of A-2b in left below corner of the diagram.

The strike of A-2 is nearly parallel with that of A-3. Moreover A-2a, and A-3a are same in the mode of movement. Therefore A-2 group were distinguished only when, (1) they are found to be older than A-3 group, or (2) they accompany A-2b set. Accor-

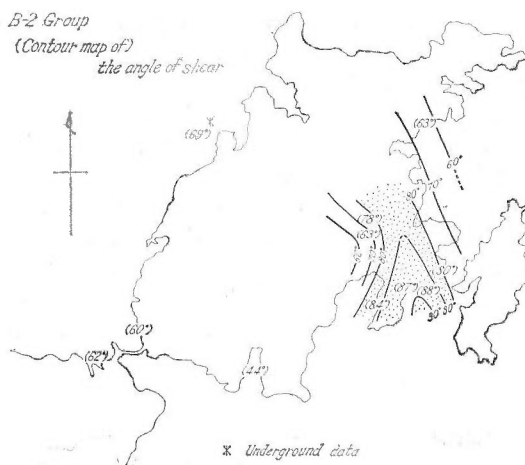


Fig. 12 Angle of shear fracture of B-2 group

dingly, it might happen, in places where time relation between A-2 and A-3 can be ascertained or A-2b set is not found, all fractures in which might contain A-2 as well as A-3 were tentatively considered as A-3 group.

A-2 set was found in Akazaki and Terashima groups and Higire group in Ōshima (Fig. 5). Most of A-2 group are found to be faults, although the displacement is small about 10 cm at most.

IV. 1. 3 A-3 group

The strike ranges between N 10° E and N 45° W. They are the fractures that are most conspicuous and of largest displacement in Terashima. Let's describe first the A-3 sets in Terashima. The mode of displacement is left lateral. The dip of comparatively large fractures is between 50° and 80° westward down, but some fractures, most of which are comparatively small, dip eastward at 75° to 80°. Apparently the former is normal fault while the latter is reverse fault. However, as shown in Fig. 18, Loc. 826, both should be considered as to be perfectly continuous and to be left lateral-slipped fractures. As shown in Fig. 17 A, average strike is N 25° W. This group is accompanied by a fracture set written as A-3bf in Fig. 17 A, the average strike of which is N 59° W with dip of 70° NE. The displacement of this fracture is of either left lateral or right lateral.

A-3 group are found also near Ōtawa east of Yobuko Strait, where the rocks dip slightly westward, and as going to the east, the lower formation is found. Here the dip of A-3 changes from westerly dip by the Yobuko Strait to easterly dip in the east.

Similar change is seen from Terashima to Ōshima in west of the Yobuko Strait. In Terashima, most of A-3 group dip westward while, in Ōshima they dip eastward. The vertical change as well as such lateral change is quite systematic, that is, in the level near coal bearing beds of Matsushima group located several hundred meters deep from the surface in northwestern Ōshima we can find both westerly and easterly dip. It can be summed up that A-3 group have westerly dip in the neighborhood of the Yobuko Strait or in Akazaki and Terashima groups. While as going away from the Strait, or as coming in the rocks of Nishisonogi group, A-3 group is changing their dip to eastward.

Concerning to the slicken side, most indicate the plunge of $N 40^{\circ} SE$. Some slicken sides, although they are a few, are nearly vertical. In some fault-planes, both plunges are found like an example of Loc. 821.

It is difficult to find the true nature of the displacement of A-3 group, because of the lack of sufficient information. It might be better to consider about that in Terashima, where information about A-3 is comparatively rich.

A-3 group should not be considered to be extension fracture. As shown in Fig. 18, A-3 group are moved step by step in left lateral direction in spite of dips. Seven poles of fractures in the right of Fig. 18 change continuously. With this reason A-3 group might be considered single plane of shear fracture. If it is shear fracture, the mode of displacement suggests that the direction of maximum principal stress shall be NNW or



Fig. 13 Distribution of C group

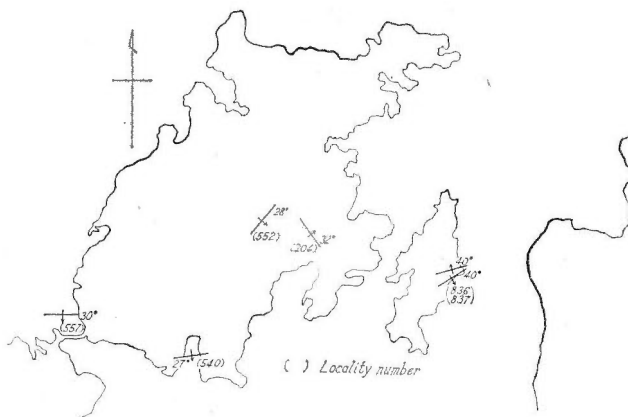
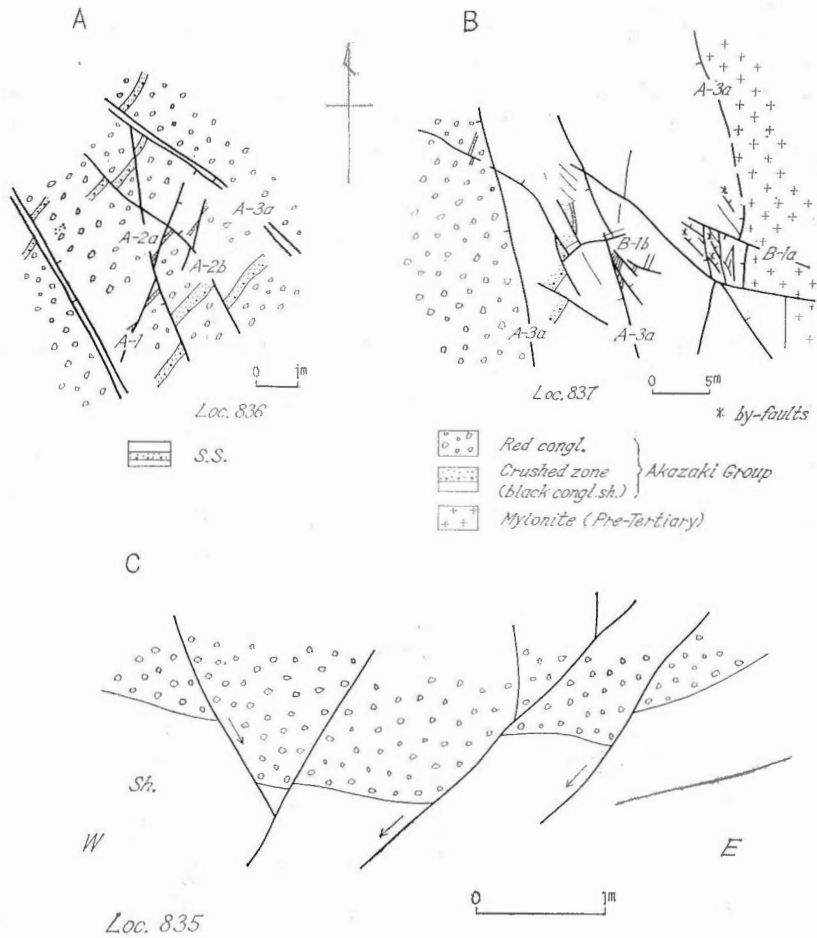


Fig. 14 Distribution of D group



A; It is shown that A-2 set makes a conjugate, and A-2 is older than A-3, but later than A-1 group. A part of the right-upper corner is shown also in plate 4. horizontal view.

B; Fracture pattern in Loc. 837, where a faulted zone running between pre-Tertiary mylonite and Akazaki group is exhibited as three major faults as shown in the figure. They all, belonging to A-3a set are of apparently left lateral and are older than B-1 set. horizontal view.

* by faults that are named A-3 bf in fig. 17 A.

C; A Conjugate set represented by A-2a and A-2b. vertical view.

Fig. 15 Occurrence of A and B-1 sets in Akazaki group, the eastern coast of Terashima.

NW. First, we can use the direction of the slicken side to decide it. It was already mentioned that there are two kinds of slicken side in A-3, vertical and 40° SE. If vertical slicken is presumed of A-3, A-3 group should be of dip slip, which goes not agree with the observation that all A-3 is of left lateral strike slip. It is possible that vertical slicken side was formed at the same time as B-2 group. Secondly, we try to take an assumption the net slip of A-3 group directed 40° SE. The procedure to decide maximum principal stress using N 40° SE slicken side is shown in Fig. 17 B-1, in which fracture group A-3a is represented by the pole of A-3a, then, we draw a great circle of the pole (a, b), and draw the direction of 40° SE of the slicken side on the great circle. Now the point that will be found at a length of 90° degree from the point of the slicken side on the great circle is the direction of medium principal stress med. (1) in Fig. 17. If we draw a great circle (c, d) at right angle to the medium principal stress, maximum and minimum principal stresses will come upon this great circle. Supposing the angle of shear 50° or 60° , the point of $1/2(180^\circ - 150^\circ) = 65^\circ$ or $1/2(180^\circ - 60^\circ) = 60^\circ$ from the pole of A-3a is the direction of maximum principal stress max. (1) in Fig. 17. Q-1 and Q-2 show presumed poles of shear fracture that is pair to A-3a.

Instead of considering A-3 group as single planes of shear, let's take an alternative idea that the fault of average strike 59° W, A-3bf in Fig. 17 accompanied by A-3a group is another plane of shear fracture making a conjugate set with A-3a set. In high pressure experimentation it is often observed single plane of shear fracture is accompanied in opposite side by another single plane of less in magnitude, forming an apparent conjugate

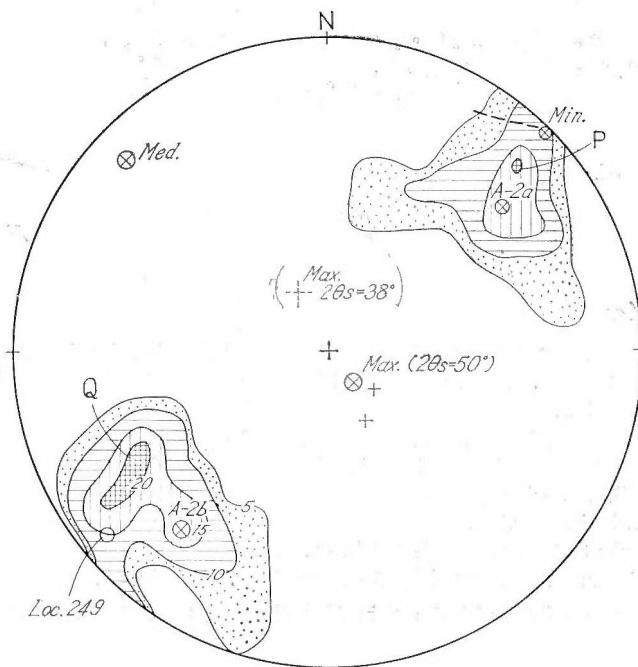


Fig. 16 Schmidt net diagram made with 20 fractures of A-2 group in Terashima. Contour line: 5-10-15-20%. There are two peaks of concentration, one represents A-2a, the other A-2b. Principal stresses are found as shown.

set. In Fig. 17, B2, principal stresses were found out with this way using A-3a and A-3bf as two poles of the conjugate set. In this case, angle of shear is 58° , the direction of slicken side is 48 SE. The principal stresses found in those two different way agree with each other as shown Fig. 17 A. Max. (1) is the maximum principal stress found in the former method, while max. (2) is that found in the latter method, and so on. It is also interesting that two maximum principal stresses agree with the poles of beddings respectively. Therefore, it seems probable that maximum principal stress at the time of A-3 group is around the area that is by three points of max. represented in Fig. 17 A.

The observation in Loc. 835, 836 and 837 indicates that A-3 group cut A-2 group (Fig. 15) and, it seems that A-3 is more fresh and larger in both length and width than A-2. In most places in Terashima and Ōshima, A-3 is older than B sets. In Fig. 19, the poles of A-2 and A-3 group are plotted into a diagram. The poles of A-2a and A-3a come down as nearly same place. Both A-2a and A-3a are same in mode of movement and of left lateral. A half of A-2b and A-3a' overlap each other, however the mode of displacement is different. A-3a' is of left lateral. The reason why conjugate set was not formed at the time of A-3 group is attributed possibly to the change of geological environments from the time of A-2 to that of A-3. The dip of the bedding was getting steeper from the time of A-2 to that of A-3, and it is probable that this change is due to the uplift movement of Terashima. The previous results of high pressure experimentation indicate that in high confining pressure the rocks are ductile and easily make conjugate set.

IV. 2 B group

It is the largest set in Ōshima. In Terashima, however it is less conspicuous than A group. B group are also found numerously in Ōtawa. The strike trends approximately WNW - ESE to WSW - ENE. They are divided into two sets according to the mode of displacement.

IV. 2. 1 B-1 group

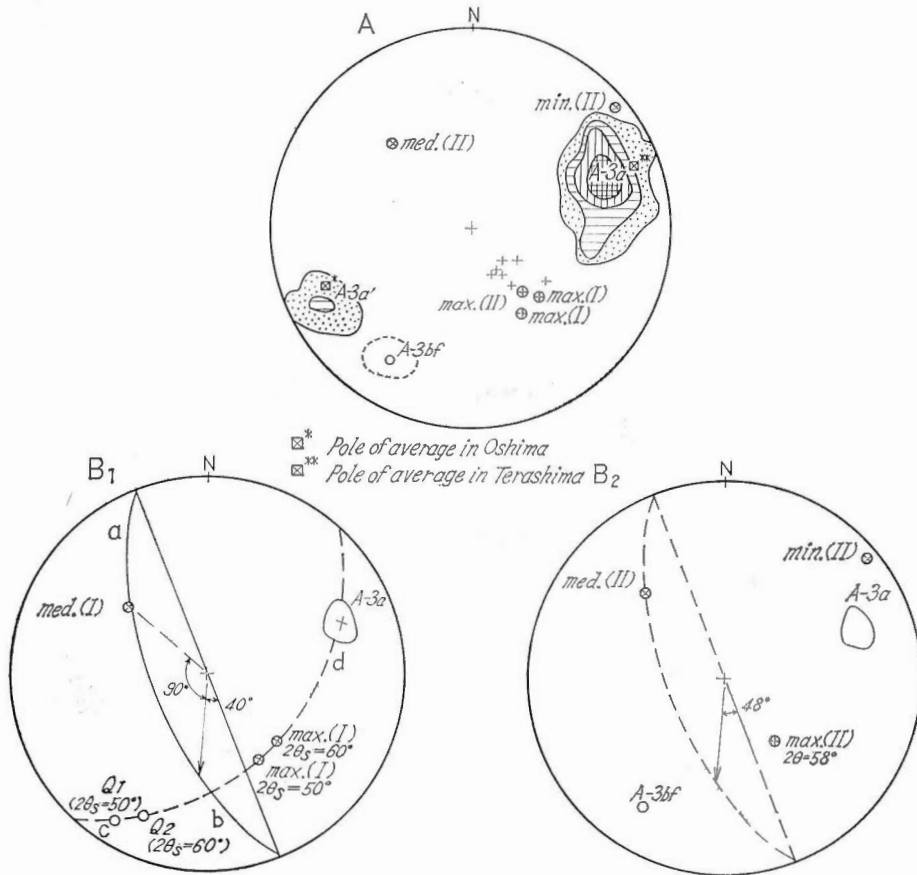
In many places, there co-exist the fractures of $N 60^\circ$ to $80^\circ W$ in strike called here B-1a group and the fractures of $N 65^\circ$ to $75^\circ E$ in strike called here B-1b. The dip of B-1a is 70° to $85^\circ N$ down in most places, but 70° to $90^\circ S$ down in a few places. The dip of B-1b is variable in places ranging $80^\circ N$ down to $75^\circ S$ down.

It is probable that B-1a and B-1b form a conjugate set because (1) both are of same age and (2) the mode of movement is strike slip, B-1a of left lateral and B-1b of right lateral. Let's consider these reasons further.

Field occurrence of B-1 group

B-1a and B-1b are not found in the same frequency and magnitude, but B-1a is much more numerous and conspicuous, as shown in faults in the geological map (Fig. 2) and the structural map (Fig. 3). The large faults of B-1a are found almost in whole area, Ōshima, Terashima and Ōtawa, while those of B-1b found only in the areas from Noda, Hamaguri to Magome, central Terashima and Ōtawa. In a extent as small outcrops, it is very rare that B-1a and B-1b co-exist and cut by each other, but one of both only is found. Let's see the examples of the connection of the both.

Fig. 20 A, B include comparatively large area. In such a extent, as coming to the



A, Contour lines were made with 48 fractures of A-3 in Terashima. Although we have two peaks, A-3a and A-3^b separately, the both belong to a set genetically as explained in the text and Fig. 18.

B₁; A-3a set has slicken side of N 40° SE. Upon presumption that this slicken side is real trace of movement along the A-3a plane, principal stresses were found on the diagram. Angle of shear was presumed 50° and 60°.

B₂; A-3a is accompanied by the smaller fracture A-3bf as shown in Fig. 15B. Principal stresses were found in alternative way by presuming that A-3a and A-3bf makes a conjugate set.

We see principal stresses from two different solutions are in good accordance in figure A.

Fig. 17 Schmidt net representation of A-3 group.

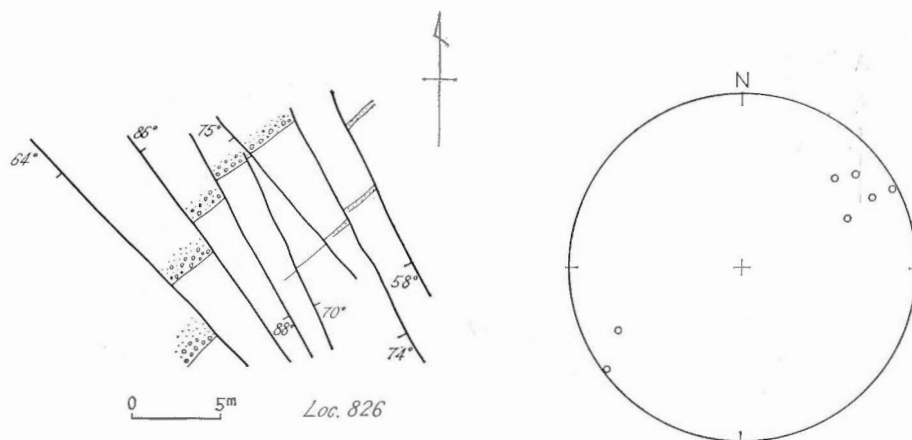


Fig. 18 Left; left lateral movement of A-3a group shown by seven faults in Loc. 826.

Right; Schmidt net presentation of the seven faults. It is shown A-3a makes left lateral slip in spite of dip-side.

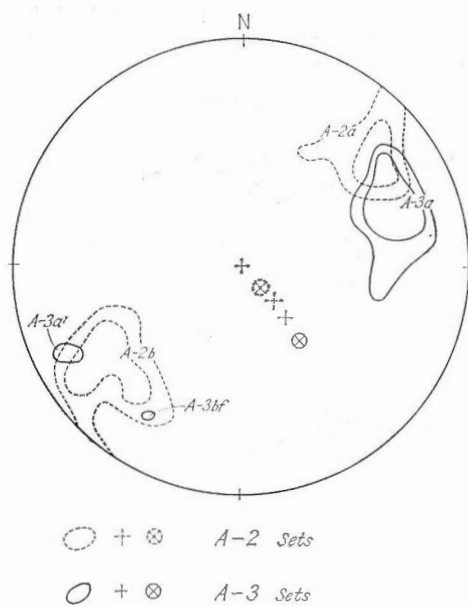


Fig. 19 Peaks and principal stresses of A-2 and A-3 groups are drawn together from Figs. 16 and 17A in a diagram for comparison.

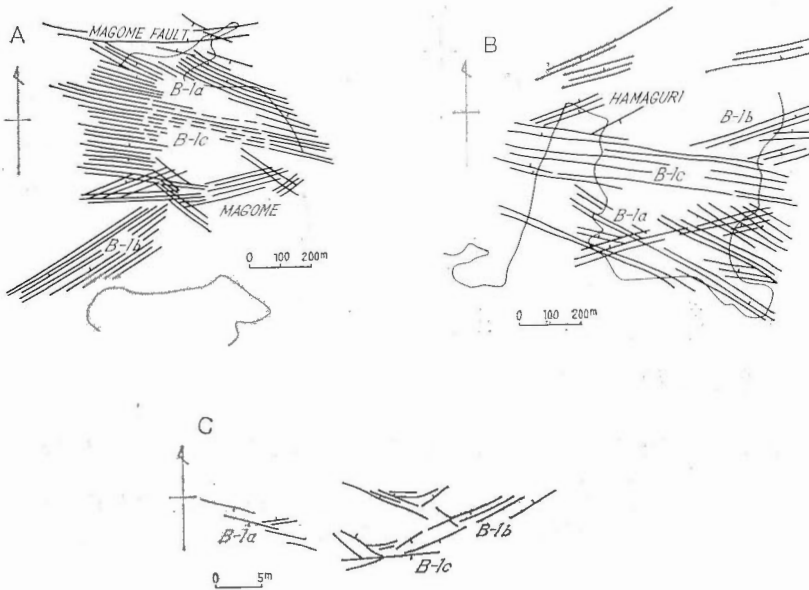


Fig. 20 Mode of occurrence of B-1 group; (1) spatial relation among them.
A, B, representation with larger scale, in central and southern Ōshima.
C. with more detailed scale, in Ottawa.

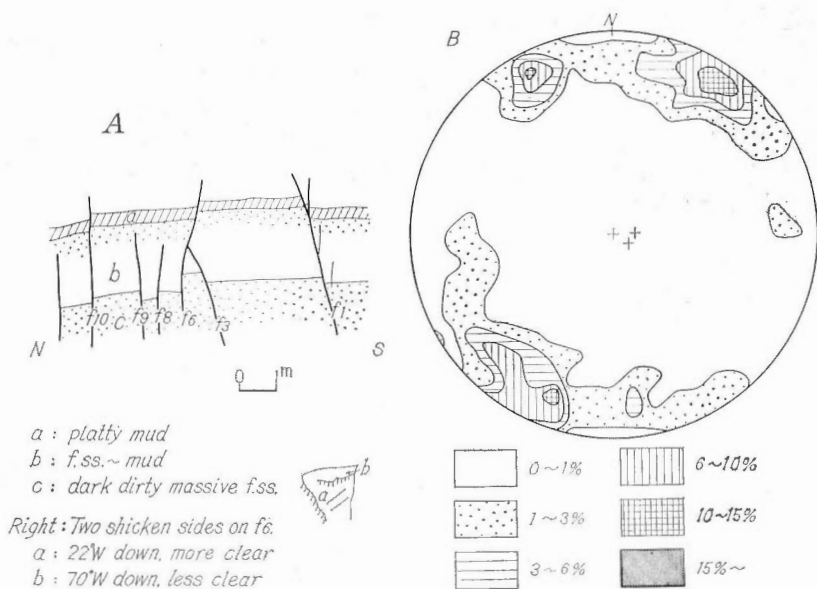
Table 3 Mode of movement and classification of minor faults at Shioda,
northwestern Ōshima.

Locality	fault number	fault strike	fault dip	plunge of slicken side	apparent vertical movement	apparent lateral movement	apparent classification	fracture set
	f 6	62°W	81°S	22°W ⊙ 70°W ○	North Side -down	Left Lateral	Reverse fault	Bla
537	f 9	53°W	79°S	20°E	N-up	LL	Normal fault	a
	f10	62°E	87°S	40°E	South Side -up	Right Lateral	Rv	b
	f 1	65°W	68°S	80°E	N-up	LL	Nr	a
	f 3	60°W	61°S	80°W	N-up	RL	Nr	a
536 535	f 3	68°W	80°S	56°W	N-up	RL	Nr	a
	f 1	62°W	78°N	57°W	N-down	LL	Nr	a
	f 6	60°W	77°S	horizontal	N-up	LL	Rv	a
424	f 3	60°W	76°S	horizontal	N-up	LL	Nr	a
	f13	53°W	78°N	horizontal	N-up	LL	Nr	a

place of the connection, the angle of shear fracture becomes smaller, then, the fractures parallel to the maximum principal stress or the direction of bisector of B-1a and B-1b occur. The last fractures are considered as so-called extension fractures and will be called here conventionally B-1c set. Further let's-see the connection in more detailed scale. Fig. 20 C would be a good example. In such good area that continuously the rocks can be observed, if we see small area such as several meters in width, probably we found one of B-1a and B-1b only there. If we go on next place to next without losing that fracture set, suddenly it looks to disappear, then the other set appears at next place. If we see around carefully, there are always B-1c group between the both groups. As seen in Fig. 20 C, the pole of B-1c is very close to the minimum principal stress. In plate 5, one more example is shown. There is found B-1c group between B-1a and B-1b like in Fig. 20 C. In a few places, B-1a and B-1b occur in network pattern cutting each other. Such field occurrence indicates that B-1a and B-1b are of the same age although they are different in frequency and magnitude.

The mode of displacement of B-1 group

B-1 group is found as joints in most places, while in some places such as shown with thick red lines in Fig. 7 it is found as faults. In order to study the mode of displacement, the area around Shioda was chosen. Fig. 21 A shows an example of the outcrops of B-1 faults. Table 3 shows the results of the measurement of slicken side on 10 faults in this area. Among 10 faults, 4 are indicated dip slip by slicken sides, but 3 of the 4 has low dip less than 78. Fault No. 6 at Loc. 537 has both dip slip and strike



A. Vertical view of the faults of B-1 group, and sketch of slicken side of fault No. 6 in Loc. 537, Shioda. refer to table 3.
 B. Schmidt net representation of 61 minor fractures in Shioda.
 Fig. 21 Mode of occurrence of B-1 group; (2) genetical relation between B-1a and B-1b. in Shioda, northwestern Ōshima.

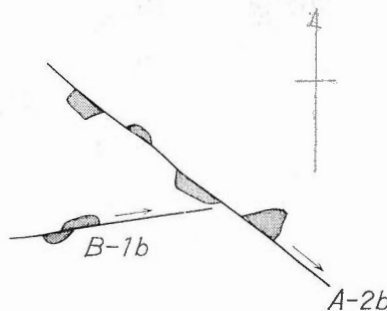
slip, (Fig. 21, A). Most of the faults that have dip of more than 76° are strike slip faults ranging 0 to 22 in plunge. By analysing the direction of slicken side and the inclination of strata, the mode of deformation for each fault was found as the seventh column from the left in the table. The five steep faults of B-1a all are of left lateral, while one of B-1b is of right lateral. In this connection, the 4 faults of low dip all are normal faults of dip slip.

In the places where B-1a and B-1b cross each other in network pattern, B-1a is of left lateral and B-1b of right lateral.

An example is shown in plate 6. In Terashima, the mode of movement is observed directly better than in Ōshima because of the existence of alternate beds and the pebbles in conglomerate rocks. Without any exception, B-1a is observed of left lateral and B-1b of right lateral. The examples are shown in Fig. 15 B and Fig. 22. It is also hardly found in Terashima that B-1a and B-1b cut each other in outcrops. The above description is concerned to joints and minor faults. Concerning to the large faults it is difficult to see the mode of displacement directly. However, fortunately, drifts of the coal mines penetrated Nakado fault, so, geology and structure in the both side are well known. SAKAKURA (1964) made it clear that Nakado fault is a left lateral strike slip fault because the isopach of upper Matsushima group is shifted 700 m left lateral by the fault. It might be concluded from the above examples that originally B-1 group is the fracture dipping steep and that B-1a is of left lateral and B-1b is of right lateral. The B-1 group of low dip are probably related to the movement of B-2 group as mentioned later.

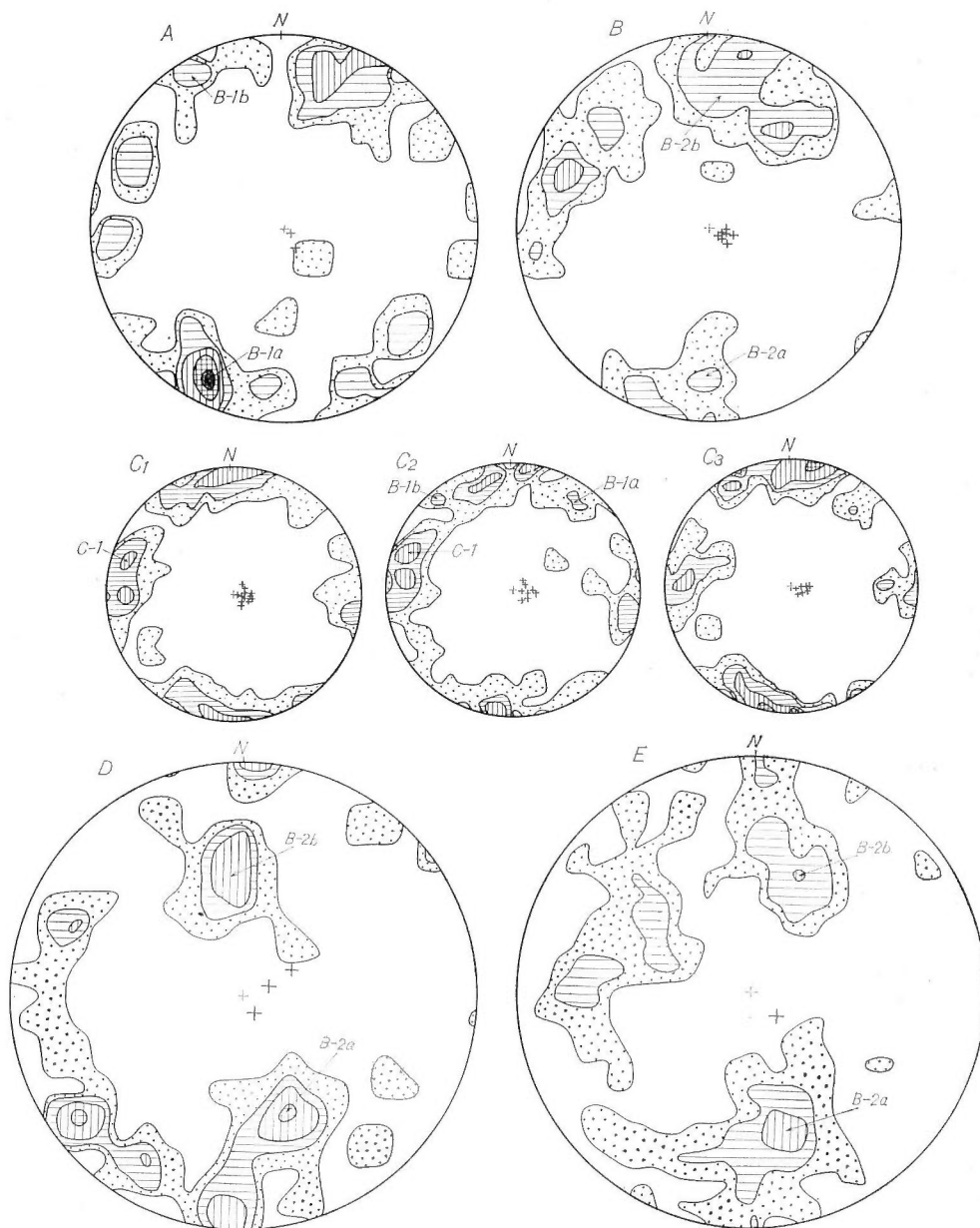
Principal stresses and the angle of shear

Fig. 8 and 9 show the maximum principal lines and the contour map of the angle of shear of B-1 group found by the method described in chapt. 3. As described in p. 19 there occur B-1c, an extension fracture near the possible intersection of B-1a and B-1b. In this area $2\theta_s$ is close to zero and it is difficult to find maximum and medium principal stress. Therefore the largest value of $2\theta_s$ in the area as large as 100 m was taken in this case.



B-1b in Loc. 832

Fig. 22 Mode of displacement of B-1b group as well as A-2b in Loc. 832, eastern coast of Terashima. The rocks are conglomerate and black area shows pebbles in conglomerate.



- A. 56 fractures, Yoko-o Pass, eastern end of Shioda fault.
 B. 128 fractures, along Magome fault.
 C. Uridake formation in Maze.
 C₁ 148 fractures
 C₂ 69 fractures in sandstone of C
 C₃ 70 fractures in alternation of s. s. and shale of C
 D. 47 fractures in Okojima.
 E. 100 fractures in Ichigojima.

Fig. 23 To show the difference and transition between B-1 group and B-2 group developing areas by Schmidt net diagrams.

In Fig. 8 medium principal stress was not drawn because of the difficulty of presentation, as it trends approximately perpendicular to the paper. Most of the plunge of the maximum stress lines are westward down. The strike of the maximum stress lines keep a considerable consistency, generally exhibiting a northward concaved curve, varying from about 88° W at the western end of Ōshima to about 85° E at the eastern end. The plunges of the minimum principal stress lines are nearly horizontal in average. It is interesting that the strike of the strata is approximately perpendicular to the maximum principal stress at all places. Accordingly the medium principal stress is nearly at right angle to the strata planes. In Fig. 39, all principal stresses of B-1 are plotted in a Schmidt net.

Next, let's discuss the result shown in Fig. 9. Comparing with the geological map and the tectonic map, it is clear that the contour map of the angle of shear is closely related to both the distribution of large faults and the rock material. Along Shioda, Umenoki and Noda the angle is between 50° and 60° , while in the area among these faults the angle is 35° to 50° . It is also found the angle is more than 50° along Magome and Tokuman faults. Concerning to the rock material, a good agreement between the angle and the rock material is also clear. The angle of shear in the area of comparatively large angle is 50° to 60° in coarse sandstone of lower Maze formation, 40° to 55° in medium to coarse sandstone of upper Maze (Janome sandstone), and 40° to 60° in medium to coarse sandstone of Shioda (Lima sandstone). Generally it is found that the angle is large in massive, medium~coarse sandstone and small in alternation. It might be right that the angle is influenced by possible geophysical factor such as suggested by the existence of the large faults more than lithological factor.

IV. 2. 2 B-2 group

B-2 group have strike of approximately E - W ranging from N 65° W to N 65° W, which is nearly same as that of B-1, but B-2 differs from B-1 in much lower dip. The dip of B-2 ranges between 45° to 60° the dip-side of which is on both northward and southward. The observation in outcrops clearly indicates the both making a conjugate set, (Fig. 25).

Most of conspicuous fractures of B-2 are found in southeastern Ōshima, where there are some large faults of B-2 group. Among the large faults, Magome fault is the largest in throw that is about 220 m at most. In southeastern Ōshima, B-2 group are found as if they took place of B-1. The fractures in point A in Fig. 1, that is located around the eastern end of Shioda fault are represented by the Schmidt net diagram of Fig. 23 A, which presents the similar pattern to that of B-1 type shown in an example at Shioda (Fig. 21 B). Further eastward, however, Shioda fault is replaced* by Magome fault and in the diagrams the pattern of B-2 type is getting clear (Fig. 23 B). This tendency is also seen in north to south direction. Going down southward, apart from Magome fault, there appear the diagram of B-1 type (Fig. 23 C) then, in the zone along Ōkojima fault, again we see the diagram of B-2 type (Fig. 23 D). It should be noted that, along these B-2 fault, joints as well as faults exhibit the character of B-2 as shown in an example of the diagram of Ichigojima (Fig. 23 E).

Important features of B-2 are both the low dip of the fracture planes and the vertical maximum principal stress suggested by dip slip movement. Recognizing these features as criterion for distinguishment of B-2, B-2 is found for almost every part in

* There have been no place that the direct connection of the two faults were observed. However a possible extension or any trace of the two faults were not found in the area beyond the presumed point of the connection.

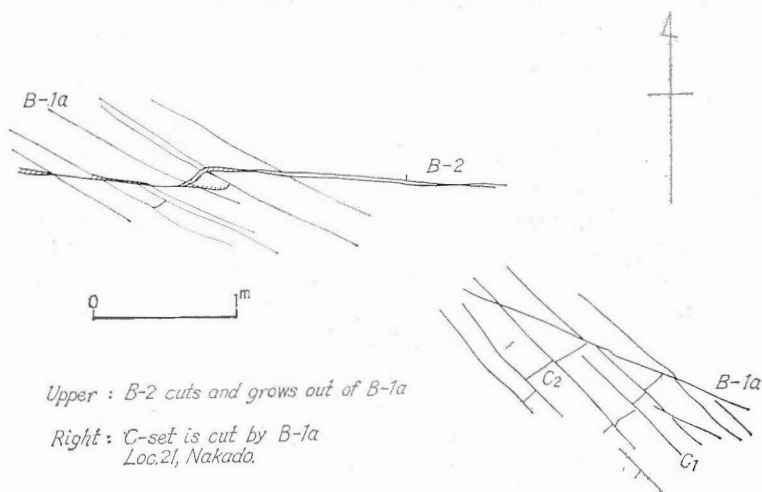


Fig. 24 Mode of occurrence of B-2 and C group at Loc. 21 in Nakado. refer to plate 7. Upper : B-2 sets intersect B-1a and grow out of it. Right : C group are proved to be older than B-1a set by being intersected by it.

Ōshima. Let's see some examples. In Fig. 24 and plate 7, we see how minor faults of B-2 are developed from B-1 joints in Nakado. It is interesting that B-2 fault has not a definite continuous plane, but B-2 grows from B-1 joints by connecting B-1 joints step by step to make planes dipping at lower angle apparently. In respect to this, an example in Shioda will be reviewed. Some normal dip slip faults having low dipping planes could be interpreted as belonging to B-2 sets. Shioda fault as shown in the geological map has a strike parallel to* these minor faults and is clearly located in the drift 700 m beneath the ground surface. If we calculate the apparent dip with the locations both in the surface and underground, we have 65° N down.

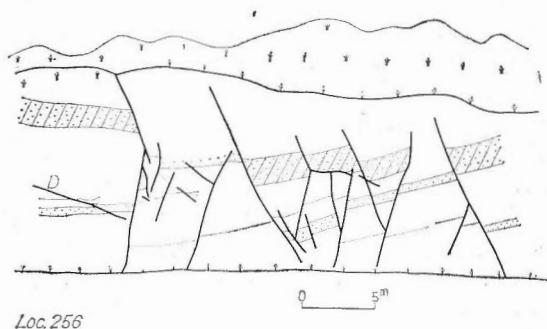


Fig. 25 A conjugate set, composed of the faults of B-2 group, Loc. 256 Maze, eastern Ōshima. D-marked is a low angle reverse fault of D group.

* The plane of Shioda fault was not observed. The fault has been presumed from the discontinuity of the rocks. Possibly it might be a fault-zone composed of parallel small faults.

It might be summarized that B-2 group have such characteristics, that, (1) the larger the degree of displacement and length is, the lower dip is, in other words, the larger the angle of shear is, and (2) they were formed as if they grow by connecting pre-existed B-1 fractures in some places. The latter characteristics indicate that B-2 is formed later than B-1 in some places. At the same time it is to remind that, in southeastern Ōshima the formation of B-1 and B-2 is dated of same age, because that B-2 seems to have taken place of B-1 and never coexists with B-1 in this area. A possible explanation for these two cases is that B-2 had been active for some long period and that at the time of the formation of B-1 vertical stress had been the largest exceptionally in southeastern part of Ōshima, then, afterwards, as stress field had changed so that vertical stress became the largest not only in southwestern part but over all areas in Ōshima so that B-2 had been formed in every part in Ōshima.

At eleven localities, principal stress lines and the angle of shear were found out (Figs. 11, 12 and 40). The maximum principal stress lines are nearly perpendicular to the bedding planes. The minimum principal stress lines have a plunge of approximately horizontal and are parallel to the strike except one locality. Medium principal stress lines are less than 10° in plunge and trend around dip direction. Thus, it is very interesting that the directions of principal stresses are closely related to the planes of sedimentation particularly in the rocks of Matsushima and lower Nishisonogi groups.

The angle of shear is much bigger than that of B-1 in most places, ranging between 60° and 80° except one. The angle is getting higher in Matsushima and Nishisonogi groups and close to 90° especially in southeastern Ōshima.

IV. 3 Other fracture groups

There are two fracture groups left for description. The both are restricted in development and much less in displacement and length than previously mentioned fracture groups.

IV. 3. 1 C group

They are closely related to the bedding planes. C-1 group is so-called longitudinal fractures being parallel to the bedding strike, while C-2 group should be called cross fractures, perpendicular to the strike. C-1 and C-2 are found always at right angle to the bedding planes. The characteristics of C group from the viewpoint of the mode of occurrence is that the planes are curved and discontinuous. This exhibits good contrast to the feature of A and B groups the fractures of which are straight and smooth for a long length. C-1 and C-2 are considered to be formed at the same time and both are dated older than B group. Some examples of the mode of occurrence are shown in Figs. 13 and 24. As shown in Fig. 24, in Nakado, each fracture in small, particularly in shale. C group is found so conspicuous in Mase that they are expressed clearly even in 1/25,000 scale map. In Mase, C group is found in massive, coarse sandstone and alternation between Mase and Uridake formations. The peak of C-1 is very clear in contour lines in Schmidt net of Fig. 23 C.

In thin shale and compact fine-grained tuff C sets have comparatively sharp fracture planes. This can be shown in Fig. 23 C3, in which we see only one peak of C-1. The close relation of C sets to the bedding plane indicates C group is extension fractures. C group is found in every formation of Matsushima and Nishisonogi groups, while there are a few in Akazaki and Terashima groups. They are found well developed especially

It is probable that D group is a result of local change of the previous stress field that caused by the fracturing of A-3, B-1, or B-2 group at the latest period of each fracturing.

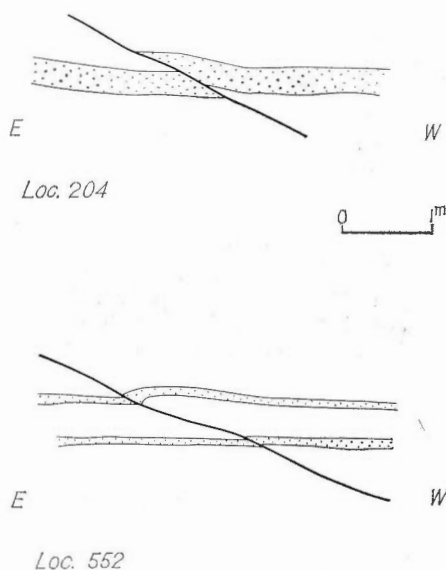


Fig. 27 The low angle reverse faults of D group. At Loc. 204, Magome and Loc. 552, near Magome Pass, central Ōshima.

V. Age of Fracturing and the Change of Stress Field

V. 1 Age of the fracture group

Time range of the fracture group is shown in Fig. 28. A-1 groups are found in Akazaki and Terashima groups only. Therefore the formation of A-1 sets is dated between Terashima and Matsushima.

A-2, A-3, B-1, and B-2 are found in the groups from Akazaki to Nishisonogi. Most of C and D groups are found in Nishisonogi. Therefore all these sets were formed after Nishisonogi. Let's consider it further in more detail. According to NAGAHAMA (1958), there are found the approximately E - W trending normal dip slip faults in Ōtawa, which cut Pliocene basalts. It is no doubt the faults are of the same group as B-2 of Ōshima. So the latest fracturing of B-2 can be dated as late as Pliocene or Pleistocene. Accordingly B-1 as well as B-2 should be also comparatively new because of genetical close relation between B-1 and B-2. A-2 and A-3 are older than B group as written in previous pages. Now as it will be described in V. 2 sudden change of the stress field from A group to B group is found indicating there might be considerable time interval between both sets. It is difficult to find the time relation between A and C. It seems any of the both does not cut the other. However, if A is later than C, we could find some place where A cuts C. On the other hand, even if C is later than A, as C is an extension fracture, apparently C hardly cuts A. Field observation indicates that the latter case is more probable. As mentioned in IV.3.1. the development of C group are closely related to that of B-2 and

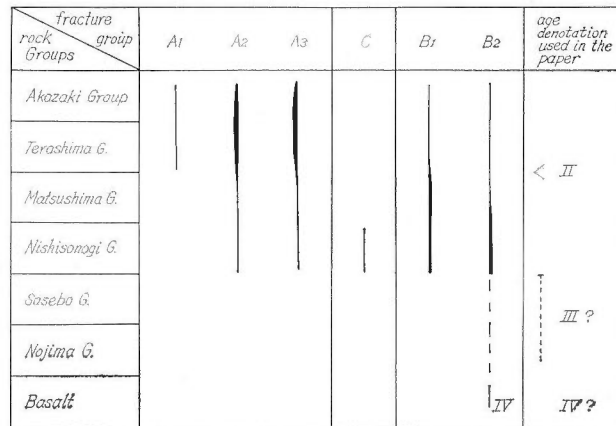


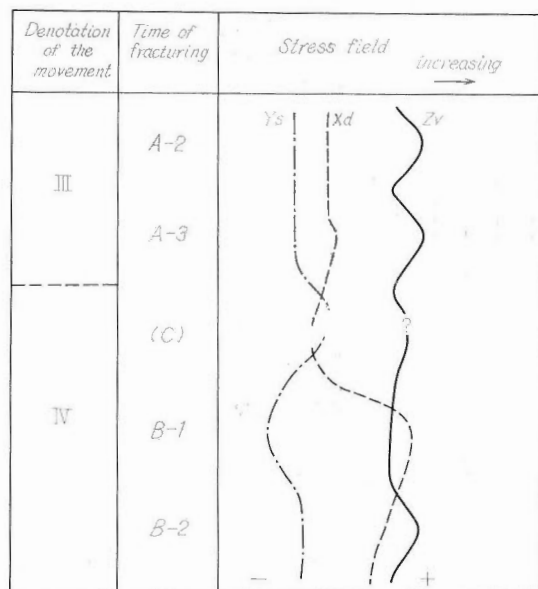
Fig. 28 Time range of the fracture group.

they are cut by B-1 at some places, therefore C group are considered to be formed a little before B group.

In neighbourhood of Sasebo, middle Miocene Sasebo group and later Miocene Nojima group are found to overlay upon the formations that are as old as Nishisonogi group, and the basaltic rocks are found over a wide area covering upon these rocks. The time of fracturings of A-2 to A-3 and B-1, B-2 should be dated among these rocks. Possibly A group would be dated as old as Miocene, and B group in Pliocene. The age of the formation of A-1 would be agreeable with the second period of Yobuko Strait fault referred by NAGAHAMA (1962). The ages of A-2, A-3, B-1 and B-2 are dated in NAGAHAMA's third period. However some revision will be made. The third period by NAGAHAMA is subdivided into two as the fracturing of A-2 and A-3 is distinguished from that of B-1 and B-2. The former shall be called the third and the latter the fourth here.

Table 4 Geometrical relation of principal stresses to bedding planes at each fracture set.

fracture group	maximum principal stress	medium principal stress	minimum principal stress	Xd : dip direction	Ys : strike direction	Zv : vertical to the beds
A-2	Zv	dip direction (N46°W)	strike direction	med. p. s.	min. p. s.	max. p. s.
A-3	Zv	dip direction (N43°W)	strike direction	med. p. s.	min. p. s.	max. p. s.
C-1	strike direction	or Zv	dip direction	min. p. s.	max. p. s.	or med. p. s.
B-1	dip direction (N86°W)	Zv	strike direction	max. p. s.	min. p. s.	med. p. s.
B-2	Zv	dip direction (N88°W)	strike direction	med. p. s.	min. p. s.	max. p. s.



Ys Strike direction
Xd Dip direction
 approximately NW-SE for III
 E-W for IV
Zv Vertical to the bedding plane

Ys, *Xd*, and *Zv* denote principal stresses, the directions of which are approximately parallel to dip-, strike- and vertical directions of the bedding at the time of fracturing respectively.

Fig. 29 Change of stress field.

V, 2 The stress fields at the fracturings during III and IV periods

It might be interesting to see how the principal stress field changes from time to time about A-2, A-3, C, B-1 and B-2, (Fig. 30).

1) Principal stress field at the fracturing of A-2, found out from the fractures in Terashima, (Fig. 16).

Maximum p. s.	N 35° W, 78° S
Medium p. s.	N 46° W, 10° N
Minimum p. s.	N 45° E, 3° E
Pole of the bedding	N 28° W, 68° S
Strike of the bedding	N 62° E

2) Principal stress field at the fracturing of A-3, from the fractures in Terashima, (Fig. 17 B2).

Maximum p. s.	N 38° W, 52° SE
Medium p. s.	N 43° W, 36° NE
Minimum p. s.	N 41° E, 6° NE
Pole of the bedding	N 37° W, 62° SE
Strike of the bedding	45° E

3) Principal stresses for C group.

Maximum p. s.	} right angle to the bedding strike- or dip- direction
Medium p. s.	
Minimum p. s.	

- 4) Principal stress field at the fracturing of B-1, average at 98 localities, (Fig. 39 A).
 Maximum p. s. N 86° W, 14° W
 Medium p. s. N 25° W, 74° E
 Minimum p. s. N 1° E, 6° S
- 5) Principal stress field at the fracturing of B-2, average at 10 localities in Ōshima, (Fig. 39 B)
 Maximum p. s. N 82° E, 80° E
 Medium p. s. N 88° E, 9° W
 Minimum p. s. N 1° W, 0°
 Pole of the bedding N 87° W, 80° E
 Strike of the bedding 3° E

As shown the above and in the figures, the directions of principal stresses are closely related to the bedding planes; A-2 and A-3 related to those of Akazaki and Terashima groups. and B-1, B-2 and C related to those of Nishisonogi. It is very interesting that three principal stresses are parallel either to the strike or dip or pole of the bedding planes within the deviation of 20 degrees. In this connection, the three directions, that is, normal to the bedding, parallel to the strike, and parallel to the dip are taken as the ordinate for each fracture set. The three directions are termed here *Zv*, *Ys* and *Xd*. With using this

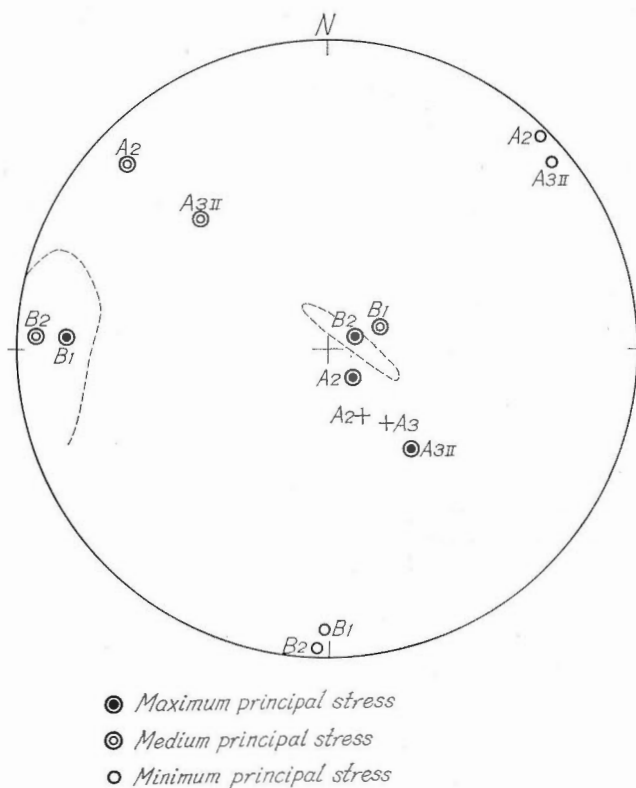


Fig. 30 Schmidt net representation of principal stresses of A-2, A-3, B-1 and B-2 group.

ordinate, the change of stress field during A-2, A-3, C, B-1 and B-2 fracturing is shown in Table 4. Except B-1, maximum principal stress is perpendicular to the bedding planes, medium is parallel to the dip direction and minimum is parallel to the strike direction. In the case of B-1, the dip direction is for maximum principal stress and the direction perpendicular to the bedding is for medium, maximum and medium are changed each other compared with the previous cases.

Concerning the directions Xd and Ys , a distinct difference exists between A and B groups. As for Xd , it trends N 36° or 45° W at the time of A, but changes to E - W in trend at the time of B. A contrast between Akazaki - Terashima groups and Matsu-shima - Nishisonogi groups is also presented by change of bedding plane in the structural map, Fig. 3. The close relation of the stress field to the bedding planes is remarkable especially in the case of A-2 and A-3 in Terashima. This could indicate that the stresses what had caused the fracturing of A-2 and A-3 would have originated in Akazaki and Terashima groups in Terashima. Quantitative representation of the change of stress field from A-2 to B-2 was made from Tab. 4 and shown in Fig. 29.

V. 3 The Yobuko Strait faults and the tectonic history in Ōshima area

The close parallelism between A group and the Yobuko Strait fault clearly indicates the genetical relation between both. From the characteristics of A-1 group, the nature of the faulting of the Yobuko Strait faults at the second period is interpreted to be the reverse faults, approximately 20° E in strike, 70° eastward down in dip, east side apparently upward. This agrees with the result that NAGAHAMA found out from the stratigraphic study.

The nature of the faulting at the third period would be more complicated. According to the cross section by NAGAHAMA, the east side comparatively goes down. Among A-2 and A-3 group, the faults along which the east side goes down are A-2 only. Provided that the author's interpretation concerning the time relation and characteristics of A-2 and A-3 in the previous pages is right, the following history along the Yobuko Strait at the third period would be possible. The structurally most important fault, for the first time, was the normal fault having the planes of N 48° W in strike and 72° E in dip (A-2 group) which was the result of the maximum principal stress of N 20° W, 70° S. Then A-3 group became active, and the faults, approximately N 15° W in strike, 80° W in dip moved of left lateral sense by the maximum principal stress which in NNW - SSE in strike, almost same as of A-2, nearly horizontal in plunge. The deformation along the Yobuko Strait faults perhaps was of the greatest, and the present geological structure would have been formed at this time. In other words, the Yobuko Strait faults had been formed as the normal faults trending NE - SW at the place as they are at the present during the early time after Nishisonogi, then there were the left lateral faults trending N 15° W. Therefore in the later time during the third period, the Yobuko faults would have been the strike slip faults being apparently normal faults. The present large throw along the Yobuko faults was possibly happened by the upward movement at the fourth period mentioned next.

It seems likely that during the fourth period when B group might have been formed, the stress field changed remarkably and the place of fracturing removed into Nishisonogi so that the movement of deformation was no longer related to the Yobuko fault. However, detailed study of the development of B-2 group indicates that there were still the effect of Yobuko faults, directly or indirectly. B-2 group are very predominantly in Magome and

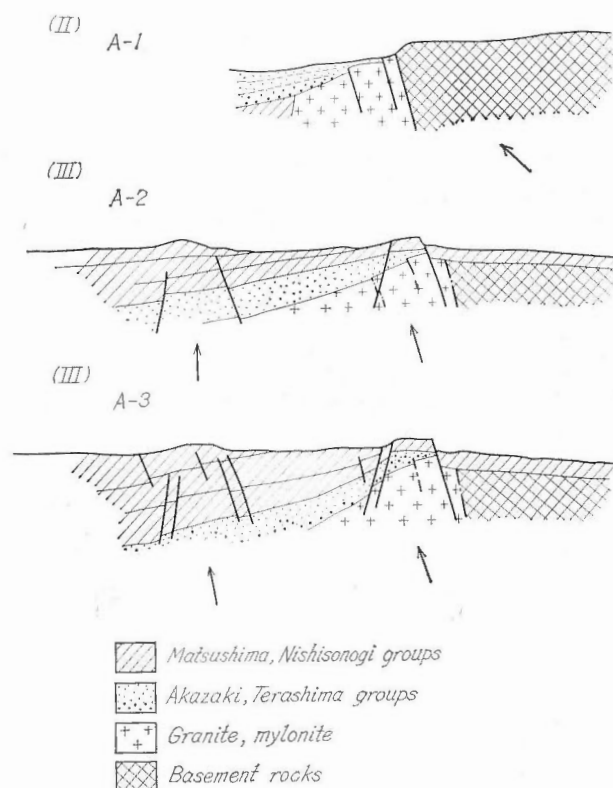


Fig. 31 Idealized cross sections of the Yobuko Strait faults and the neighbourhood.

Maze in southeastern Ōshima. The area in which B-2 group develop conspicuously extends from Magome and Mase to Ōshima-machi. According to the subsurface information that includes direct observation with the wall rocks in the coal mining drifts, B-2 is found in Matsushima group in Ōshima-machi, northwestern Ōshima, several hundred deep from the ground surface. The fractures of B-2 here are observed to be faults having the angle of shear of approximately 70° . On the other hand, from Ōshima-machi to Mase is the zone that A-3 is so predominant, (Fig. 38). The zone from Ōshima-machi to Mase trends $N 20^\circ$ to $30^\circ W$ and is nearly parallel to the strike of A-2 and A-3. This indicates that there existed the kind of horst or the faults parallel to the Yobuko faults in the rocks beneath Ōshima-machi - Mase zone (possibly in the pre-Tertiary rocks or Akazaki and Terashima), and that these buried structural features had become active during the fourth period as the Yobuko faults were active in the third period.

It is also noticeable that there is a gentle syncline trending approximately $N 30^\circ W$ in the anticlinal axis in Kurose, northeastern Ōshima. The idealized sketch showing the tectonic development along the Yobuko faults is shown in Fig. 31.

VI. The Boundary Stresses at the Fracturing of B-1 Group

VI. 1 Introduction

In the previous chapter, the history of principal stress fields was discussed from the change of the fracture pattern of A-2, A-3, B-1 and B-2 groups. Generally it is not so difficult to find out the average principal stress fields from the fracture pattern, but it might be difficult to find the complete solution of the boundary stresses. If the boundary stresses are known and the criterion of fracturing is given, we are able to draw the trajectories of principal stresses with the method as shown by HAFNER, W. (1951) and SANFORD, A. R. (1959), but generally it might be impossible to go the reverse way to find out a definite boundary stresses from a stress distribution pattern. Nevertheless, if a quantitative solution is obtained for this problem it could provide a good basis for comparison of various explanations that have been presented for better understanding of the cause of the joints.

The principal stress line of B-1 group is expressed by a simple and regular curve. B-1 group contains the most typical joints, and found most extensively than any other sets, and, so, it could be one of the keys to make the cause of the jointing clear up. In this chapter a trial will be done to calculate the boundary stress at the fracturing of

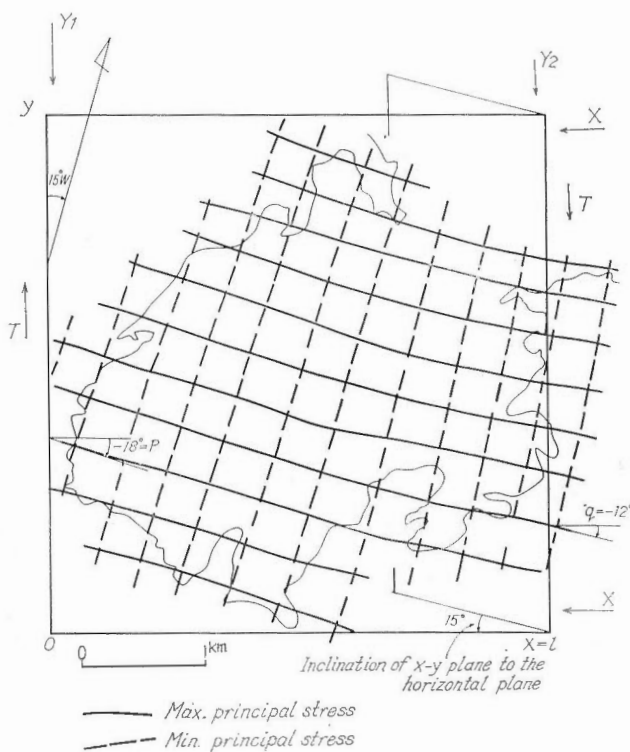


Fig. 32 The model of boundary stress analysis.

B-1 from the maximum principal stress trajectories as shown in Fig. 8 using Airy function method upon the assumption that the deformation was elastic up to the fracturing point. Yet, in result absolute value of each boundary stress could not be found out. However, by introducing Mohr's criterion, the result was given that the minimum principal stress (Y_s) must be tensile stress.

VI. 2 Calculation upon the assumption of elastic and brittle deformation

1. The following items are presumed.
 - (1) The deformation of the rocks is elastic up to the yield point.
 - (2) The fracturing is made according to Mohr's criterion.
 - (3) The maximum principal stress trajectories are represented as the curve shown in Fig. 32, and under the coordinate in Fig. 32 the problem can be treated as the two dimensional problem.

2. For simplicity, a model of Fig. 32 was set up. Y axis is taken in the direction of $N 15^\circ W$, X axis in $N 75^\circ E$ and Z axis inclining to 75° eastward, then maximum and minimum principal stresses are approximately parallel to $x - y$ plane. The average curve of the maximum principal stress trajectory is shown like that in Fig. 32. The problem is now what boundary stresses produce this curve.

3. In the case of two dimensions, the condition in which stress components σ_x, σ_y^* and τ_{xy} keep elastic equilibrium is given by finding out Airy function Φ that will satisfy the formula

$$\frac{\partial^4 \Phi}{\partial x^4} + 2 \frac{\partial^4 \Phi}{\partial x^2 \partial y^2} + \frac{\partial^4 \Phi}{\partial y^4} = 0 \dots\dots\dots(6-1)$$

by the formula

$$\begin{aligned} \sigma_x &= \frac{\partial^2 \Phi}{\partial y^2} \\ \sigma_y &= \frac{\partial^2 \Phi}{\partial x^2} \\ \tau_{xy} &= - \frac{\partial^2 \Phi}{\partial x \partial y} \dots\dots\dots(6-2) \end{aligned}$$

Here, it is presumed that σ_x, σ_y and τ_{xy} are linear function of x only because the maximum principal stress trajectory changes little along y axis.

Now, provided that Φ is a homogeneous cubic equation of x, y , then the equation

$$\Phi = \frac{a_1}{6} x^3 + \frac{b_1}{2} x^2 y + \frac{c_1}{2} x y^2 + \frac{d}{6} y^3 + \frac{e}{2} x^2 + f x y + \frac{g}{2} y^2$$

satisfies equation (6-1)

Then, from (6-2)

$$\begin{aligned} \sigma_x &= cx + dy + g \\ \sigma_y &= ax + by + e \\ \tau &= -bx - cy - f \dots\dots\dots(6-3) \end{aligned}$$

Here, the coefficient of y must be zero, because of the previous assumption that the stress components are a linear function of x , that is, $d=b=c=0$

So,

$$\begin{aligned} \sigma_x &= g \\ \sigma_y &= ax + e \\ \tau_{xy} &= -f \dots\dots\dots(6-4) \end{aligned}$$

* Compressive stress is positive.

If the boundary condition in the model co-ordinate in Fig. 32 is termed as $\sigma_x = X$, $\sigma_y = Y_1$ when $x=0$, $\sigma_y = Y_2$ when $x=l$, and $\tau_{xy} = T$, then

$$\begin{aligned} \sigma_x &= X \\ \sigma_y &= Y_1 + (Y_2 - Y_1) \frac{x}{l} \\ \tau_{xy} &= -T \end{aligned} \dots\dots\dots(6-5)$$

Formula (6-5) gives stress components σ_x , σ_y , τ_{xy} at any point (x) in the model co-ordinate in Fig. 32.

4. If z is the angle that the maximum principal stress makes with x axis,

$$\tan 2z = \frac{2\tau_{xy}}{\sigma_x - \sigma_y} \dots\dots\dots(6-6)$$

adding(6-5),

$$\begin{aligned} \tan 2z &= \frac{-2T}{(X - Y_1) - (Y_2 - Y_1) \frac{x}{l}} \\ \tan 2z &= \frac{-2T}{(X - Y_1) - (Y_2 - Y_1) \frac{x}{l}} \end{aligned}$$

now,

$$\begin{aligned} h &= \frac{(X - Y_1)}{(Y_2 - Y_1)} \\ k &= \frac{2T}{Y_2 - Y_1}, (Y_2 - Y_1) \neq 0 \\ \tan 2z &= \frac{k}{\frac{x}{l} - h} \end{aligned} \dots\dots\dots(6-7)$$

it is written in this way

$$y = \frac{k}{m - h} \dots\dots\dots(6-7)'$$

where

$$y = \tan 2z, m = \frac{x}{l}$$

This is hyperbola, the origin of which moves $h=m$. Here, k and h can be found out from the trajectory of the maximum principal stress in Fig. 32, that is, if

$$z = p, \text{ when } x=0, \text{ or } m=0$$

$$z = q, \text{ when } x=l, \text{ or } m=l$$

$$\begin{aligned} h &= \frac{\tan 2q}{\tan 2q - \tan 2p} \\ k &= \frac{\tan 2q \times \tan 2p}{\tan 2q - \tan 2p} = h \tan 2p \end{aligned} \dots\dots\dots(6-8)$$

From the trajectory in Fig. 32, we get $p=18$, $q=-12$, then $h=-1.58$, $k=+1.14$.

5. The Mohr's criterion is expressed in the formula (see Appendix)

$$\begin{aligned} \sigma_m^2 &\geq \sigma \sin \varphi + T_0 \cos \varphi, \text{ for } \sigma_m \geq \frac{1 + \sin \varphi}{\cos \varphi} T_0 \\ \sigma_m^2 &\geq 2 \tan \varphi (1 + \sin \varphi) T_0 \sigma + \frac{(1 + \sin \varphi)(1 - 2 \sin \varphi)}{(1 - \sin \varphi)} T_0^2, \\ &\text{for } \frac{1 + \sin \varphi}{\cos \varphi} T_0 \geq \sigma_m \geq \tan \varphi (1 + \sin \varphi) T_0 \end{aligned} \dots\dots\dots(6-9)$$

here, $\sigma_m \frac{1}{2} (\sigma_1 - \sigma_3) = \sqrt{\frac{1}{4} (\sigma_x - \sigma_y)^2 + \tau_{xy}^2}$

$$\sigma = 1/2(\sigma_1 + \sigma_3) = 1/2(\sigma_x + \sigma_y)$$

T_0 : shearing stress

φ : angle of internal friction

adding (6-5) and (6-7), (6-9) can be written as follows.

for $(Y_2 - Y_1) \geq \frac{2(1 + \sin \varphi)}{P \cos \varphi} T_0$

$$Y_1 \leq 1/2 \left(\frac{P}{\sin \varphi} - Q \right) (Y_2 - Y_1) - T_0 \cot \varphi$$

for $\frac{2(1 + \sin \varphi)}{P \cos \varphi} T_0 \geq (Y_2 - Y_1) \geq -\frac{2(1 + \sin \varphi)}{P \cos \varphi} T_0$

$$Y_1 \leq \frac{P^2 \cot \varphi}{8(1 + \sin \varphi)} (Y_2 - Y_1)^2 - \frac{Q}{2} (Y_2 - Y_1) - \frac{\cot \varphi (1 - 2 \sin \varphi)}{2(1 - \sin \varphi)} T_0$$

for $\frac{2(1 + \sin \varphi)}{P \cos \varphi} T_0 \geq (Y_2 - Y_1)$

$$Y_1 \leq 1/2 \left(\frac{P}{\sin \varphi} + Q \right) (Y_2 - Y_1) - T_0 \cot \varphi \dots\dots\dots(6-10)$$

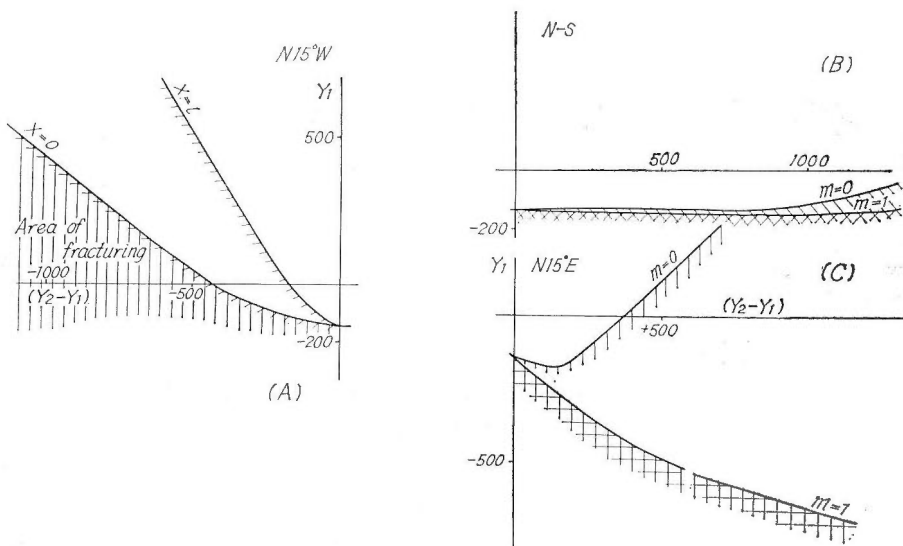
here, $P^2 = (h - m)^2 + k^2$

$Q = h + m$

6. We know $h = -1.58$, $k = 1.14$. Moreover, using the figures $\varphi = 40^\circ$, $T_0 = 300$ kg/cm²

from (6-10), the relation $(Y_2 - Y_1)$ and Y_1 is found out as shown in Fig. 33 A. The area plotted with oblique lines is that what fracturing can occur according to Mohr's criterion, formula (4-9).

7. According to Fig. 33 (A), Y is negative or tensile stress for $(Y_2 - Y_1) > -460$ kg/cm. For $(Y_2 - Y_1) > -460$ kg/cm, Y_1 is positive or compressive stress and represented with formula, $Y_1 = -360 - 0.8 \times (Y_2 - Y_1)$ approximately. If $-100, -150, -200$, and -500 kg/cm of $(Y_2 - Y_1)$ are given, X, Y_1, Y_2 , and T are calculated as Table 5.



A ; Y-axis is N 15° W B ; Y-axis is N-S C ; Y-axis is N 15° E.

Fig. 33 Area of possible fracturing as results of the calculation.

Table 5 Possible boundary stress as results of calculation.

$Y_2 - Y_1$	-100	-150	-200	-500
X	60	160	250	750
Y_1	-100	-80	-70	50
Y_2	-200	-230	-270	-450
T	-55	-80	-110	-280

unit : bars

VI. 3 Geological implication of the result of calculation

Let's discuss whether the three items that were presumed for the calculation are reasonable or not.

a) On the model of elastic and brittle deformation; The high pressure deformation tests by HANDIN and others (1957, 1958, 1963), BRACE (1964), DONATH (1964) and MOGI (1964, 1965) indicated that the sedimentary rocks such as sandstone and shale are brittle up to the confining pressure of 1,000 bars and the breaking or yield points almost agree with the elastic limit. High pressure experimentation of representative rocks of Ōshima and its neighbourhood was conducted by the author (K. HOSHINO, in preparation). Results of two kinds of rock will be given in Appendix 2. We see the rocks in Ōshima area are more brittle and have larger strength than the rocks of same age in other countries. The confining pressure of 1,000 bars equals to the overburden pressure at the depth of about 4,000 m. There would be little possibility that thicker rocks than 4,000 m were above Nishisonogi group.

b) On Mohr's criterion; Any theory of the failure of rocks have not been established absolutely right yet, however, Mohr's theory might be best for the failure of the porous rocks. The Mohr's criterion says that the loss of cohesion will occur and the rocks are fractured when the ratio of shearing stress τ_n to normal stress σ_n along the planes attains to a definite point, that is, $\tau_n \geq f(\sigma_n)$. Recently, BRACE (1960, 1964) thought that if tensile stress around the both ends of the microfractures existed in the rocks increases more than a certain value, these microfractures are connected next to next continuously and then macroscopic fracturing will occur. However even if this idea is admitted, the condition for failure will be expressed by the same formula, $\tau_n \geq f(\sigma_n)$.

Generally, linear function is used for the function $f(\sigma_n)$. However, the results of recent deformation tests show the Mohr's envelope is nearly linear under the confining pressure beyond 500 or 100 bars, while the curve differs from the linear under the pressure less than 500 or 100 bars. Therefore, combined envelope, as formula (6-9) was used in this paper. For $\sigma_n \geq 0$, the Mohr's envelope is expressed as linear and for $\sigma_n < 0$ it is expressed as parabola. Putting $\varphi = 40^\circ$, $T_0 = 300$ bars into (6-9), the failure condition is shown as in Fig. 34.

c) On the modeling of the maximum principal stress; To have the trajectory of maximum principal stress as a function of x only might be reasonable because that the trajectory exhibits little change along y direction. The form of linear function was taken for simplicity of the calculation. The simplicity of this order would not affect the geological interpretation of the result of calculation. In previous pages the trajectory was treated as hyperbola and h and k are found out. To compare the modeled curve with a real one, the modeled curve is shown in Fig. 35 by putting $h = -1.58$ and $k = +1.14$ into form (4-7).

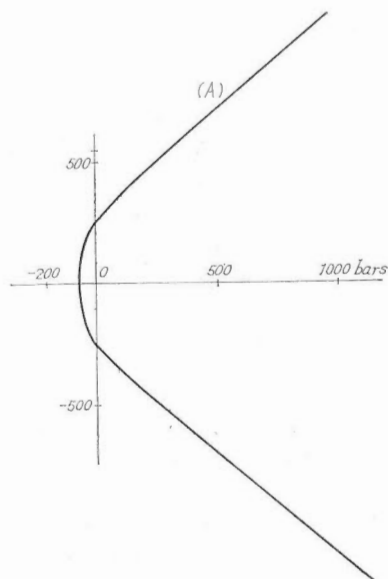


Fig. 34 Curve of formula (6-9), parabola-linear presentation of Mohr's failure criterion, when φ is 40° and T is 3,000 bars.

d) On taking y axis $N 15^\circ W$; The minimum principal stress of B-1 sets trends approximately north to south. The general trend of the strike in central Ōshima is around $N 15^\circ E$, which is nearly parallel to the Yobuko faults during the second period. On the other hand, there were a zone of uplift or faults running in the direction $N 30^\circ W$ in Nishisonogi group in central Ōshima during the fourth period or the time of B-2 group, as explained in V.3. The trend of $N 30^\circ W$ is the same as that of the strike in

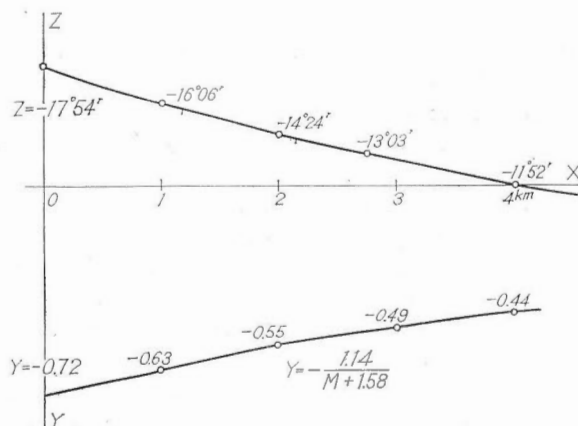


Fig. 35 Below: curve of formula (6-7), when $h = -1.58$, $k = +1.14$.
Upper: maximum principal stress line reproduced from the curve below for comparison with the stress line of the model in Fig. 32.

northern and southern Ōshima. As B-1 is closely related to B-2 in age and in space of fracturing, so this zone probably existed in the time of B-1. The trend of the Yobuko faults during the 3rd period was around N 15° W. Therefore we see the Yobuko faults, which possibly, had been the most important structural fracture in the Ōshima area through the fracturing of A-1 to B-2 or through the second, third and fourth periods, changed their directions N 15° E in the fracturing of A-1 N 15° W in that of A-2 and A-3 and possibly N 30° W in that of B-2. In the time of B-1, the trend would have been between N 15° W and 30° W. From this matter, the y axis was considered to be N 15° W. Moreover, along N 15° W, the points of the most concaved on the trajectory are found as if they are connected on a straight line. However, in addition, the results of the cases of N 15° E, 0° as y axis are shown in Fig. 33 B and C. In the latter two cases, Y_1 is in negative area, as in the case of N 15° W, but in contrast, being $(Y_2 - Y_1) > 0$, so towards the west tensile stress must be bigger. This does not agree with the geological data. Therefore, in conclusion, the direction of around N 15° W as y axis would be good, as far as the present geological data concerned.

Next, let's discuss the geological implication that should be involved in these figures and the calculation, provided that these results were right.

1. $(Y_2 - Y_1) < 0$, or $Y_2 < Y_1$; This relation is supported by geological data. The stress field of B-1 and B-2 was considered something as that under the stress field, in which considerable lateral compressive stress acted regionally, vertical compressive stress due to the upward movement was getting bigger and bigger. In such circumstances, as the upward movement continues, the rocks make lateral expansion and apparently tensile stress will come out. This tensile stress must be bigger in the area in which upward movement is stronger, therefore it should be $Y_2 < Y_1$. Also Y_s axis, the minimum principal stress of B-1 should be parallel to the axes of the upward movement. This is also proved from Fig. 11 of principal stress map of B-2.

PRICE (1959) calculated tensile stresses which could be come out during the upward movement. According to him, for 1 km of a relative uplift, approximately 110 bars of tensile stress will work, if Young's modulus is 7×10 kg/cm. In the case of Ōshima, the distance between $x=0$ for Y_1 , $x=l$ for Y_2 is about 4 km, and the difference of the upward at two points might be not so much, therefore $(Y_2 - Y_1)$ is estimated, actually, -100 bars at the most.

2. On the value of Y ; The result of the calculation indicates that Y_1 is possibly tensile stress. This might be supported by the conclusion of the previous discussion. B-1 group are found predominantly in Nishisonogi, the thickness of which is approximately 600 m. Under the circumstances without any tectonic stress, if vertical stress equals to overburden rock pressure, the vertical stress is estimated around 150 bars (240 bars/km). Even if the base of Nishisonogi is presumed in more depth, for instance, as deep as 1,500 m the vertical stress will be about 360 bars.

Generally, lateral stress in elastic equilibrium condition is given as $\sigma_x / (m-1)$, where m is poisson number. If m is 8, Y_1 is 20 or 50 bars. As PRICE (1959) stated, the uplift of 1,000 m will be resulted tensile stress of 110 bars, therefore it is understood that Y_1 actually can be tension.

3. On the value of X ; Detailed study of the distribution of B-1 and B-2 sets indicates that in the area Ōshima-machi to Maze, there is the boundary of the both sets at lower Nishisonogi or Matsushima groups, thus, where σ_x should be equal to σ_z approximately. Presumably, σ_x is constant regardless of depth, then X equals to σ_z approximately. Because the level of lower Nishisonogi or Matsushima is located 400 to 800 m deep, σ_z

is around 100 or 200 bars if it all comes from overburden pressure. σ_z may be larger, if there is the tectonic stress by upward movement or there is additional overlying rocks of considerable thickness. Therefore X must be more than 100 or 200 bars.

4. T represents strike slip component along $N 15^\circ W$, y axis of the model. It was already described that the Yobuko Strait faults which are nearly parallel to A group in trend possibly gave an influence upon the fracturing of B group. Accordingly it is suggested that this strike slip component is related with underlying faults of A group.

It might be concluded, from the previous discussion that the result of the calculation is in good agreement with geological data. However, it should be noted that the value of X is considered a little smaller than it should be if comparing with the geological data. The most appropriate boundary stresses, thus, would be around -150 bars of $(Y_2 - Y_1)$. From Tab. 5 the stresses at this condition are estimated, Y_1 equals -80 bars, Y_2 equals -230 bars, and T equals -80 .

VII. Jointing and Faulted Zones

VII. 1 The angle of shear

Because of the extensive and predominant distribution, B-1 and B-2 group are good for studying the regional variation of the angle of shear, (Figs. 9 and 12). Specifically B-1 is found in almost every outcrop in the area, so that it is the best set for seeing the change. As already written, there are found apparent influence of both tectonic and rock material factors upon the angle of shear of B-1 group. As for the tectonic factor, the angle $2\theta_s$ is found between 50° and 60° in the rocks near faults while it is between 35° and 50° in the rocks without faults. The interval of the faults is nearly same over

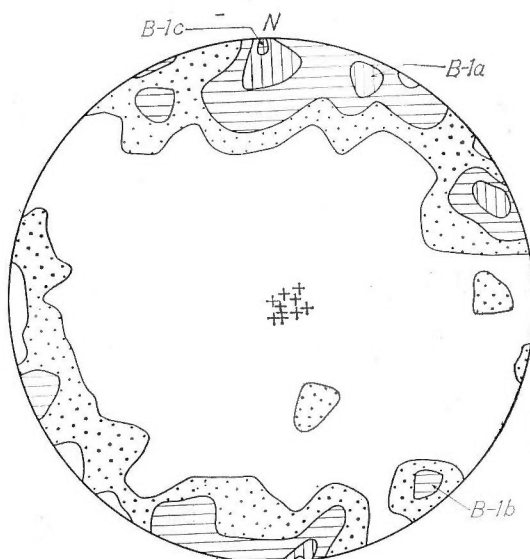


Fig. 36 Schmidt net diagram of 70 minor fractures in Ōtawa.

the whole area as shown in Fig. 7 and it is estimated about 1 km. In the rocks without faults, even minor faults are not observed and every fracture is found to be joints in terms of the definition. In other words, the distinction between faulted area and non-faulted area is clear and the angle of shear is differentiated in both areas.

The faulted area ranges 200 and 400 m in width. In the faulted area not all fractures are faults but some joints are also included. In the faulted area, the angle of joints as well as that of faults is comparatively large. Accordingly it might be probable that the faulted and non-faulted areas have been differentiated as early as the time of fracturing.

As for the other fracture sets,

A group 50° (mostly on the faults)

B group $60^\circ - 88^\circ$ (mostly on the faults)

The large value of B-2 is considered to be resulted from that B-2 group are the fractures that grew out of the formerly existed B-1 fractures. In the case of A-2, if faults only are taken for consideration, the angle is more than 50° .

According to the failure condition of Leon-Mohr, the angle of shear increases as maximum or minimum principal stress increases, (NADAI, 1950, p. 221, MUELBERGER, 1961). This relation was proved experimentally by PATTERSON (1958), BRACE (1964) and MOGI (1964). Maximum and minimum principal stresses are function of σ_x , σ_y and τ , thus the angle of shear is function of σ_x , σ_y and τ . We have seen already that, in the simplified tectonic model of Ōshima, σ_x and τ should be constant in x and y axes, and only σ_y is a function of x . We saw also that the variation of the angle of shear related to the tectonic factor seems to be quite little along x axis. Therefore it is probable that the boundary stress field gave little influence upon the differentiation of the angle of shear

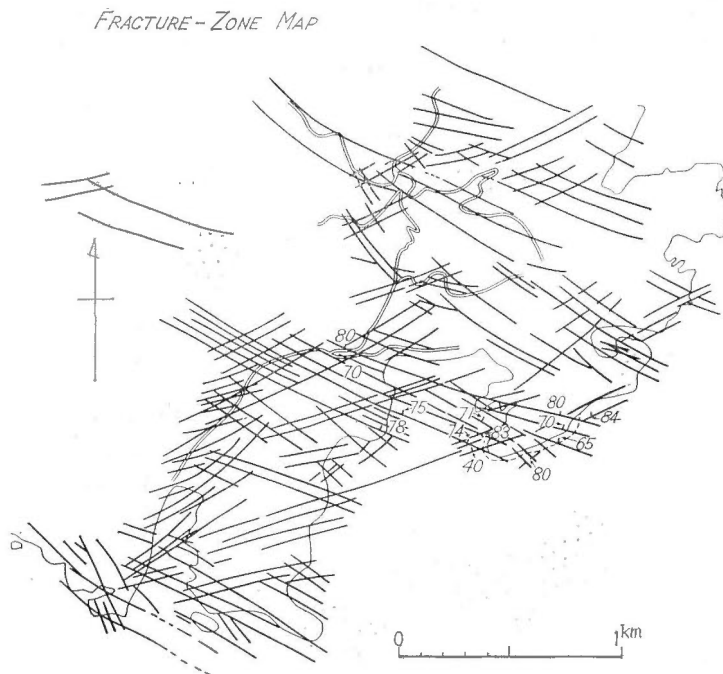


Fig. 37 Occurrence of fractured zone in southwestern Ōshima.

in deformation in Ōshima area.

The rock material would have no relation to such variation along y axis, because rock material does not change in N - S direction but does change in E - W direction.

Further consideration on the cause of the differentiation of the angle will be made in the later pages in VII. 3.

VII. 2 Extension and shear fractures

As shown in Fig. 7 and 20 C there are found B-1c, an extension fracture near the conjunction of B-1a and B-1c seems to be formed at the same or a little earlier than B-1a and B-1b. In the net diagram in Fig. 36 which was made from 70 fractures in the neighbourhood of Ōtawa, the peak of B-1c is shown stronger than those of B-1a and B-1b. In such diagrams that include area of considerable extent or some separated outcrops, the peaks equivalent to the extension fracture of this kind are usually found on a position of median line of the shear fracture. That is, shear and extension fractures are found usually together in Schmidt net diagrams, they are observed to be formed at the same time at most localities, but the phenomena that extension and shear fractures intersect each other were rarely observed. Such conjunction as shown the above differs in mode and possibly genetically from that of cross and oblique fractures described by many workers like DE SITTER (1956) or PRICE (1959). The cross fracture is equivalent to C-2 here. It is indicated in Fig. 23 C that the peak of B-1c is clearly distinguished from that C-2. Moreover B-1 group is dated latter than C group (Fig. 24). However, such relation between extension and shear fractures have been found out on B sets only so far. It was well observed especially in alternative part of sandstone and shale and the uplift zone along Ōshima-machi to Mase in Ōshima.

It is interpreted that the extension fracture of this kind is a consequence of local disturbance of strain field which made in brittle deformation near the point of intersection of shear fracture.

If a certain extent is chosen for estimation of the angle of shear and the largest value is taken in each area, the angle is nearly constant. It is structurally interesting that the relation between extension and shear fracture is same in both smaller and larger scales. In both cases the places that the angle of shear is getting zero is that two planes of shear fracture make intersection. The decrease of the angle is not continuous, but at a certain small angle, decreasing seems to be stopped then extension fracture seems to occur. In Fig. 7 a pattern of the intersection is shown in larger scale, in which, it seems likely that disturbance of strain distribution was brought out near the intersection of shear fracture, at where extension fracture was resulted to be formed.

The plane of extension and shear fractures was observed to be same. Any distinctive features could not be observed.

VII. 3 Faulted zones

Faults are always accompanied by more or less joints parallel to them. There were no faults without joints. In B-1 group, the faulted zones are found in a definite distance, approximately 1 km, (VII. 1, Figs. 7 and 38), and the parallel joints as well as faults were observed in faulted zones. Most fractures were joints and the faults were quite rare in non-faulted zones.

It might be more interesting that, even in non-faulted zones, a similar pattern exists, that is, the zones of high fracturing and the zones of little fracturing are found alternately.

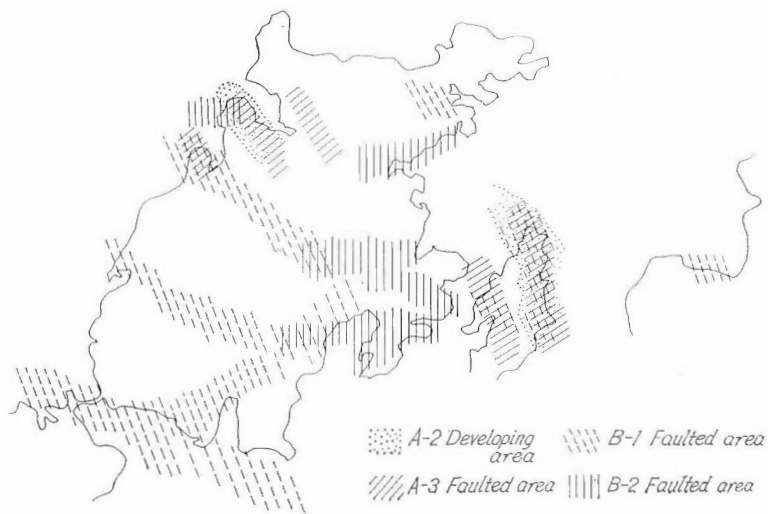


Fig. 38 Faulted or predominantly fractured areas repeated in different ages of fracturing.

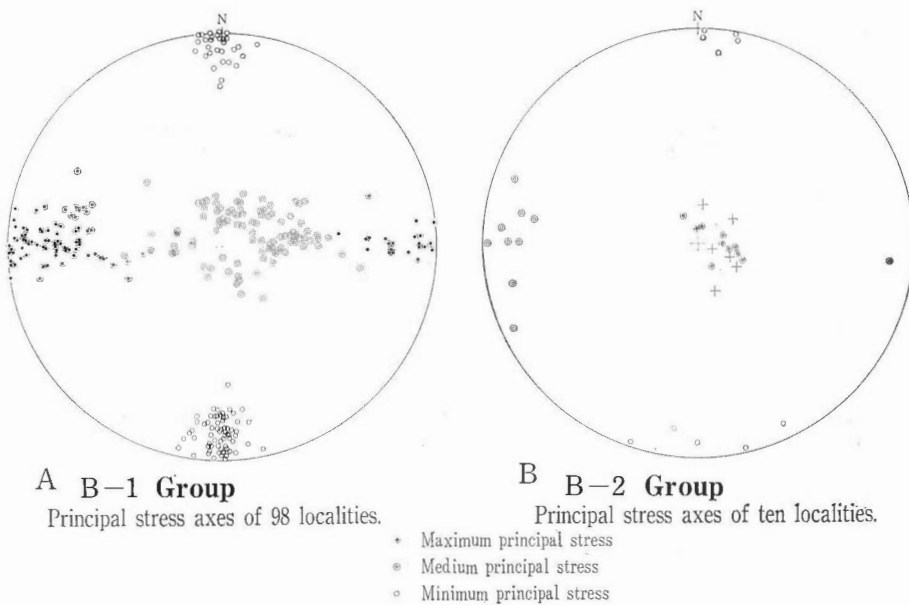


Fig. 39 Schmidt net representation of principal stresses of B-1 and B-2 groups.

In Fig. 37 is shown the fracture pattern near Magome and Maze. A particular fracture group, for instance, the joint of B-1 group develops in such mode that it is well found in some zones but it is rare in other zones. The former is called fracturing zones here. In the area through Magome and Maze, the distribution of the fracturing zones is systematic, which ranges 50 to 300 m in width and 300 to 2,000 m in distance. It was described in VII.1. that the differentiation of the angle of shear can hardly be explained by neither boundary stresses nor rock material. The area of large angle is equivalent to faulted area.

That the faulted and fracturing zones occur at some distances is considered to be similar feature as that fractures occur at distances at outcrops. Also, this might be similar as the fracture pattern in rock specimen experimentally deformed in high pressure. The distance of fractures or density of fracture experimentally made have been considered through experimentation by some workers to have relation with ductility, (HANDIN, communication). However, we have no satisfactory theory on this matter.

How the rocks are faulted relates undoubtedly to rock material. In conglomerate beds in Terashima there are a few joints, nearly all fractures were faulted. However, the factor such as rock material only is not enough to explain the above questions. The faulted zones become re-active repeatedly throughout a series of stress field, although there would be a little change in the direction of stresses. As shown in Fig. 38, the zones that A-2 group developed well in is that will have well been faulted during the fracturing of A-3, and B-2 developed well in the area that A will have made good development.

VIII. Mechanism of the Jointing in Ōshima Area

Among A, B, C and D groups, both faults and joints are included. However joints are developed very well in B group. A-3 has also well defined joints although in A-1 and A-2 faults are more predominant than joints. Finally, geological and geophysical environments favoring the jointing will be reviewed and summarized as follows and problem on mechanism of jointing will be discussed with emphasis upon B-1 group.

The joints of B-1 group

Most of B-1 is found in Matsushima and Nishisonogi groups, the rocks of which are very brittle up to 1,000 bars of confining pressure (Appendix 2). These rocks exhibit gentle isoclinal structure dipping westward at less than 10° at the angle of dip. There are no indication of violent tectonic movement, such as folds with steep dipped wings or large thrust. Field observation and the analysis of principal stresses indicates that the joints possibly were formed by the tensile stress resulted from the upward movement of the pre-Matsushima groups that occurred in a time considerably late after Nishisonogi group had become well cemented. B-1 group are found in every rocks throughout Matsushima and Nishisonogi which consist of, from below, coarse sandstone, alternation of medium sandstone and shale, and volcanic coarse sandstone being about 1,000 m in thickness. The planes of joints are sharp in most cases and have no plumose structure. The planes are apt to be curved in sandstone while linear and keep in good and dense parallelism in shale, volcanic sandstone and fine sandstone. The average interval among joints is 2 to 5 m in coarse sandstone but 10 to 30 cm in shale. The interval varies depending upon the thickness and rock material. As for the rock material, the average grain size is most important. The smaller the grain size is and the thinner the bed is, the smaller the interval is. The fracturing zones, are 300 and 700 m in average interval. This interval is

no longer affected by rock material or thickness of bed, but nearly constant over Ōshima. The interval among faulted zones is about 1,000 m, which is constant throughout Ōshima. The extent of a joint plane ranges 1 to 5 m in shale and 5 to 30 m in coarse sandstone. The extent of fracturing zones and fault-planes is about 300 or 2,000 m. These figures may indicate some relation between the largeness of the fracture and the scope of influence of stress field at fracturing. The distribution of the faulted zone agrees with the contour map of the angle of shear. The faulted zones are found in the places where the angle of shear is comparatively large.

B-1a and B-1b, two groups composing of B-1 make a conjugate set. The joints of B-1 have no direct proof to be decided as shear fracture because of no visible movement along the planes, but close relation to the parallel faults indicates they can be classified as shear joints. B-1a develops more conspicuous than B-1b. Around the area where B-1b and B-1a intersect there occur extension joints. The planes of extension joints look same as those of shear joints, no plumose structure was observed. Transition from shear joints seems to be perfectly continuous and this agrees with the conclusion BRACE (1965) found out from high pressure experimentation. Extension joints will occur as if they come out of shear joints when the angle of shear is getting small to close to zero. However if both are found together in an outcrop, such relation is often observed that the angle of shear does not change continuously but there seems to be some discontinuation. The distribution of extension joints is also closely related to contour map of the angle of shear, and extension joints are found in the places where the angle is the smallest.

Under what physical condition the fractures of B group were faulted or turned to be extension fractures in some particular areas is very interesting problem. However, it might be difficult to find out the cause of this differentiation. The variation in the initial stress field can be hardly a cause of this differentiation, if there is any variation. (see VII. 3). This differentiation might be compared with such results of high pressure and clay model deformation experimentation that, although constant stresses are added along the boundaries of the specimen, concentration of stress or strain will be produced inside of the specimen and the fractures are formed at definite interval.

The joints of B-2 group

Most of large fractures of B-2 are the faults which are recognized as conjugate set at outcrops. They are found in the area from Ōshima to Mase, central part of Ōshima. A few are found in western Ōshima, most of which does not exhibit conjugate set. The angle of shear of the B-2 faults is extraordinary high in central Ōshima. This is due partly to that B-2 was formed out of the previously existed B-1, and partly to the rotation of the planes after the fracturing. This is same in the case of joints. Therefore, the joints of B-2 differ in the mechanism of formation from that of B-1. B-2 can be described the local or later fracture pattern of B-1 group.

The joints of A-3 group

Most of the fractures of A-3 in Terashima are apparently normal faults dipping westward, while in Ōshima most are the reverse faults dipping eastward. There are two directions of slicken sides, 40° S down and vertical, and the former is considered to be primary one, thus both the normal fault in Terashima and the reverse fault in Ōshima must be strike slip faults of left lateral. Vertical slicken side is probably that what was made by the upward movement during the B-2 group.

On the other hand, most of A-3 in Matsushima and Nishisonogi groups in Ōshima

and Ōtawa are joints. This is possibly due to that Terashima is located within 1 km west of the Yobuko Strait where the Yobuko Strait faults are considered to run. However because in Nishisonogi group in Ōtawa which also located within 1 km east of the Strait there are few faults, this topographical relation is not perfect for the explanation. The difference in rock material did possibly give an affect upon this. Though there is no available experimental information, conglomerate might be ductile and easily faulted. The rocks in Terashima dip northwestward at 30° or 40° . The direction of maximum principal stress estimated from the slicken side of 40° S is nearly as right angle to the bedding plane, in Terashima, but in Ōshima there are some information which indicate the parallel movement along the bedding planes.

The joints of A-1 and A-2 can not be distinguished from that of A-3, if any, because the planes are nearly parallel.

In the above, geological and physical environments at the jointing in Ōshima area have been reviewed. Now, the characteristics of joints and the mechanism of jointing in general sense shall be discussed.

1. Joints may be either extension or shear fracture.
2. Though it is shear joint, it occurs as fracture without any visible displacement along the planes over considerable area. Most of the planes are smooth and sharp, have neither slicken side nor plumose structure.
3. Most of joint set are accompanied by parallel faults which are found as faulted zones at a definite interval. The strain at the fracturing may be released mostly along the faults. However, we know some cases in which only joint occurs in the area of several thousand km. In such cases it is difficult to explain how and where the strain that stored up to the time fracturing is released. Therefore joint should be considered to be the fractures that were formed in quite early stage that total strain is quite small yet.
4. HANDIN thought the total strain at fracturing point as an index of ductility. The failure at small total strain is formed in very brittle deformation. Experimentally sandstone are very brittle up to 500 bars of confining pressure and shale very brittle up to 1,000 to 1,500 bars. These indicate that the more brittle the rock is and the lower the confining pressure is, the more easily joints will be formed.
5. HANDIN (1963) made it clear that the relation between pore pressure and confining pressure which has been approved in soil mechanics is also recognized in rock mechanics. This means that true confining pressure is found out by subtracting pore pressure inside the specimen from the side pressure and it is most meaningful. Accordingly the state of very brittle may exist even in deep located rocks, or in high lithostatic pressure if fluid pressure in the pores is satisfactory high, as stated by SECOR (1964).
6. The joints of B-2 was interpreted to have been formed by tensile stress during the rocks underwent upward movement. We have no direct information, however, whether other fracture groups are also consequences of tensile stress or not. The strength of rocks and the tectonic history would suggest that the jointing during the upward movement is more probable than that during the downward process. Nevertheless, it is premature to conclude that all joints are a consequence of tensile stress as stated by PRICE (1959).

The confining pressure in the triaxial high pressure experimentation means the stress given around the column of the specimen, and it is minimum principal stress in compression test while it is maximum principal stress in extension test. There have been quite a little information available about extension tests comparing with compression tests. Although the relation between confining pressure and ductility, and fracture pattern in extension tests is not so clear, the results up to the present indicate that the mode of

deformation changes from brittle to ductile as confining pressure increases, as in compression tests, (BRACE, 1964; HOSHINO, unpublished data). The Mohr's envelope is drawn similar to compression. The envelope of extension test is parallel to the envelope of compression test but in most cases a little above. If such result can be applied to all cases, the deformation by tensile stress favors brittle deformation more than the deformation by compressive stress because the minimum principal stress at fracturing is extremely low in extension deformation. In the fracturing by tensile stress, the rocks will be able to have the fracture, that is more systematic, and with less displacement along the planes.

7. Fields study about the spatial relations between joints and the faulted area and between shear and extension joint suggests that the angle of shear fracture was to be determined as early as the macroscopic fractures are found out in the rocks. The area of large angle is found nearly in or near the faulted zones and that of smaller angle is approximately around the places that two sets of shear fracture intersect each other or extension fracture occurs. It is considered that such regular distribution depends upon a kind of systematic strain concentration produced within the rocks that might be formed even under uniform boundary stresses rather than under the initial differences of boundary stresses.

IX. Conclusion

The fractures found in Ōshima area are divided into A-1, A-2, A-3, B-1, B-2, C and D groups on the basis of parallelism of the planes, mode of displacement and age relation. Groups A or A-1, A-2 and A-3 are found in the sandstone and conglomerate of Akazaki and Terashima groups and most of them are minor faults. Groups B or B-1 and B-2 are mostly found in the sandstone, shale, and alternation of sandstone and shale of Matsushima and Nishisonogi groups in Ōshima. Most of B-1 are joints, while most of B-2 are faults which are found at the outcrops as conjugate set. The fracturing of A group is dated possibly in early Miocene and that of B sets are possibly in late or middle Pliocene. A-2, B-1 group were found to make conjugate set from field study. The principal stress fields during A-2, A-3, B-1 and B-2 group are shown in Tab. 4 and Figs. 28, 29, which indicate that the co-ordinates of stress field in A and B groups differ greatly. As for the horizontal component, northwesterly and northeasterly trends in A group turned to approximately northerly and easterly trends in B group. This indicates that there were at least two tectonic movements after the time of Nishisonogi group.

Nishisonogi group, in which B-2 group are found numerously and predominantly consists of very brittle sedimentary rocks, about 600 m in thickness and ranging Oligocene to early Miocene in age. It exhibits a gentle structure with isoclinally westerly dip, less than 10 degree. B-2 group are formed originally as shear fracture having 40° to 50° in average acute angle, the maximum principal stress of which trends approximately eastward or westward. B-2 is actually found as closely spaced and little shifted joints with good parallelism. At the same time, B-2 group are faulted at interval of about 1 km. The faulted zone contains many minor faults being parallel one another. The faults of B-1a are of left lateral and those of B-1b are of right lateral. The both faults partly changed to apparent normal dip slip faults by later vertical movement. The faulted zones are mostly in the area of large angle of shear. Differentiation of the angle of shear fracture is considered to have existed as early as the initial fracturing begin. On the other hand, in the middle between two faulted zones are found the area of small angle of shear, where two sets of shear joint make intersection and extension joint prevails. Such differentiations

of faulted zones and extension joint area are comparable with some results of experimentation in mode of appearance.

Maximum, medium and minimum principal stresses of B-1 are approximately E - W, vertical and N - S respectively, (Figs. 11 and 39). Its principal stress lines are represented by simple and regular curve, (Figs. 11 and 32). Using this curve, under the presumption that the fracturing was done by ways of elastic deformation up to the breaking point and by Mohr's criterion on failure the boundary stresses at B-1 group were calculated by using Airy function. The result of the calculation indicated that the minimum principal stress is tensile stress. The fractures of B-1, both joints and faults, thus, are considered to have been formed by approximately north to southerly tensile stress resulted from upward movement.

It might be concluded that so-called joints are the fractures that are formed as a result of very brittle deformation. Very brittle deformation is favored in such circumstances that brittle rocks like hard shale, tuffaceous argillaceous rocks or massive hard sandstone are fractured under low confining pressure. In such deformation, the strain when the fracture is formed is so small that the displacement along the planes can be hardly visible. If it is in the circumstances that the strata is moving upward and tensile stresses are easily resulted, brittle deformation will be favorable so much and in such cases the development of systematic joints over a large area will be made possible.

Appendix 1: The equation of failure condition

If maximum principal stress is σ_1 and minimum principal stress is σ_3 , (σ is positive if it is a compression) Mohr's criterion for linear equation is expressed as

$$\sigma_m \geq \sigma \sin \varphi + \tau_0 \cos \varphi \dots\dots\dots(10-1)$$

where φ is angle of internal friction, τ_0 shearing stress and σ_m and σ are given as

$$\sigma_m = \frac{1}{2}(\sigma_1 - \sigma_3), \quad \sigma = \frac{1}{2}(\sigma_1 + \sigma_3)$$

If it is expressed for parabola,

$$\sigma_m^2 - 4d\sigma \geq 4d(\alpha - d) \dots\dots\dots(10-2)$$

where d is focal distance and α the distance between maximum point of parabola and the origin of co-ordinate. Now, if graphs represented by (10-1) and (10-2) touch at the point $\sigma_3 = 0$ or $\sigma = \sigma_m$, and (10-1) is used for $\sigma_3 > 0$, (10-2) used for $\sigma_3 < 0$, then

$$d = \frac{1}{2} \tan \varphi (1 + \sin \varphi) \tau_0$$

$$\alpha = \frac{(1 - \sin \varphi)^2 (1 + \sin \varphi)}{2 \sin \varphi \cdot \cos \varphi} \tau_0$$

Adding them to (10-1) and (10-2),

$$|\sigma_m| \geq \sigma \sin \varphi + \tau_0 \cos \varphi \dots\dots\dots(10-3)$$

$$\sigma_m^2 \geq 2\sigma \tau_0 \tan \varphi (1 + \sin \varphi) + \frac{(1 + \sin \varphi)(1 - 2 \sin \varphi)}{(1 - \sin \varphi)} \tau_0^2 \dots\dots\dots(10-4)$$

Thus we get formula (6-9). If we put $\sigma_m \leq \sigma$ in (10-3), we get

$$\sigma_m \geq \frac{(1 + \sin \varphi)}{\cos \varphi} \tau_0$$

Now, in (10-2), σ_m has minimum value when $\sigma_m \geq 2d$ (NADAI, 1960), then

$$\sigma_m \geq \tan \varphi (1 + \sin \varphi) \tau_0$$

Accordingly, (10-3) and (10-4) can be applied respectively for the scope shown in the following equations.

$$\sigma_m \geq \frac{1 + \sin \varphi}{\cos \varphi} \tau_0$$

$$\frac{1 + \sin \varphi}{\cos \varphi} \tau_0 \geq \sigma_m \geq \tan \varphi (1 + \sin \varphi) \tau_0$$

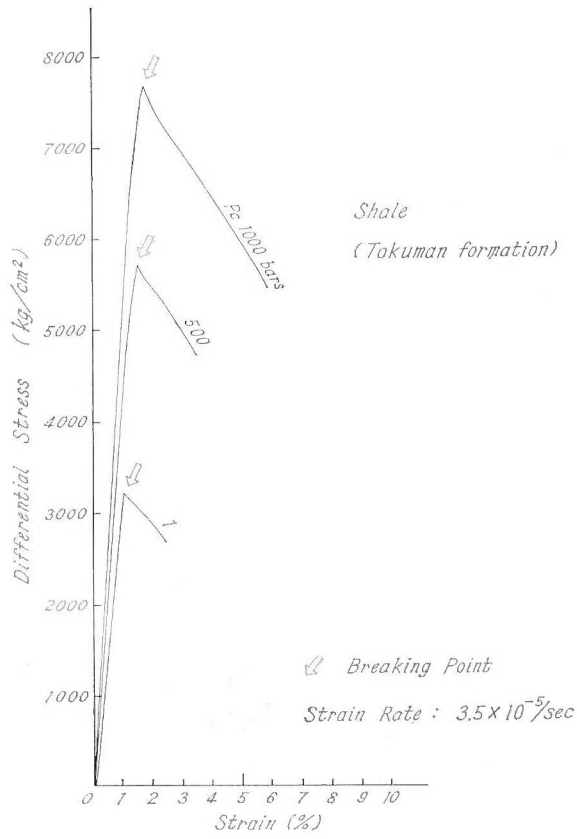


Fig. 40

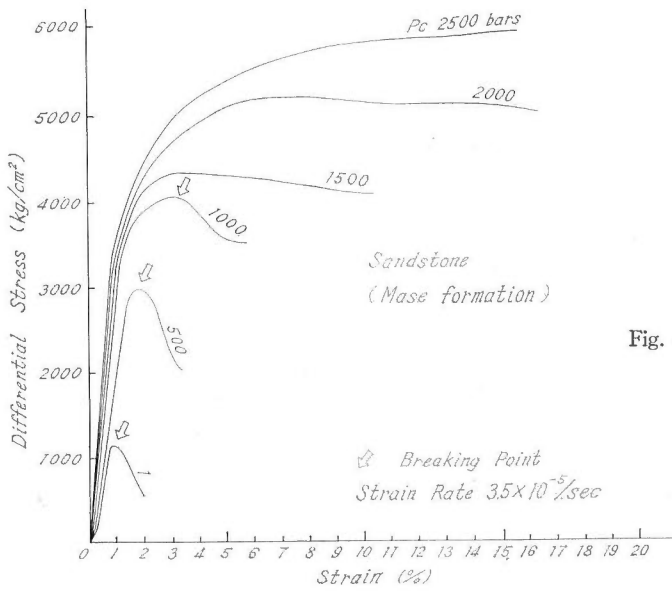


Fig. 41

Appendix 2: Results of triaxial experimentation

Results of two kinds of rock from Ōshima area are given in Figs. 40 and 41. The experimentation was done of dry samples. The size of which is 19.5 mm in diameter and 39.0 mm in length. These two are representative rocks of those that produced in Ōshima area. Shale in Fig. 40 is probably most brittle rock and sandstone in Fig. 41 is most common in the area.

References

- BADGLEY, P. C. (1965): Structural and tectonic principles, A Harper International Student Reprint, Harper Row, New York.
- BEZUHOV, N. I. (1953)*: Theory of elasticity and plasticity, TOSUDRS, Moscow, translated into Japanese by T. Sato and published by Nikkan-kogyo-shinbun-sha.
- BILLINGS, M. P. (1954): Structural geology, Prentice-Hall, Inc.
- BRACE, W. F. (1960): An extension of the Griffith theory of fracture to rocks, Jour. Geophysical Research, vol. 65, p. 3477-3480.
- BRACE, W. F. (1964): Brittle fracture of rocks. State of stress in the earth's crust, Am. Elsevier Publishing Co., Inc.
- BUCHER, W. H. (1920-21): The mechanical interpretation of joints, Jour. Geol., vol. 28, p. 707-730, vol. 29, p. 1-28.
- DE SITTER, L. U. (1956): Structural geology, McGraw-Hill Book Co., Inc.
- DONATH, F. A. (1964): Effect of loading rate on the deformational behavior of rocks subjected to triaxial compression, NSF report.
- GRIGGS, D. & HANDIN, J. (1960): Observation on fracture and a hypothesis of earthquakes, Geol. Soc. Am., Memoir 79, Rock deformation, p. 347-364.
- HAFNER, W. (1951): Stress distribution and faulting, Bull. Geol. Soc. Am., vol. 62, p. 377-388.
- HANDIN, J. & HAGER, R. V., JR. (1957): Experimental deformation of sedimentary rocks under confining pressure: Tests at room temperature, Am. Assoc. Petroleum Geologists Bull., vol. 41, p. 1-50.
- HANDIN, J. & HAGER, R. V., JR. (1958): Experimental deformation of sedimentary rocks under confining pressure: Tests at high temperature, Am. Assoc. Petroleum Geologists Bull., vol. 42, p. 2892-2934.
- HANDIN, J. & other, (1963): Experimental deformation of sedimentary rocks under confining pressure: Pore pressure tests, Am. Assoc. Petroleum Geologists Bull., vol. 47, p. 717-755.
- HARRIS, J. F. & others, (1960): Relation of deformational fractures in sedimentary rocks to regional and local structure, Am. Assoc. Petroleum Geologists Bull., vol. 44, p. 1853-1873.
- HEARD, H. C. (1960): Transition from brittle fracture to ductile flow in Solenhofen limestone as a function of temperature, confining pressure, and interstitial fluid pressure, Geol. Soc., Memoir 79, Rock Deformation, p. 196-226.
- HODGSON, R. A. (1961a): Regional study of jointing in Comb Ridge-Navajo Mountain area, Arizona and Utah, Am. Assoc. Petroleum Geol. Bull., vol. 45, p. 1-38.
- HODGSON, R. A. (1961b): Reconnaissance of jointing in Bright Angel area, Grand Canyon, Arizona. Am. Assoc. Petroleum Geol. Bull., vol. 45, p. 95-108.
- HOSHINO, K. (1962)*: Calculation of fracture porosity from measurements at surface exposures, with an example on Tertiary sedimentary rocks in the Hiki Hills, Saitama Pref., Jour. Jap. Ass. Pet. Tech., vol. 27, p. 181-191.
- HOSHINO, K. (1963)*: Joint system of the Kushiro Coal Field, Jour. Jap. Ass. Pet. Tech., vol. 28, p. 238-245.
- HOSHINO, K. (1965a): Fracture system and natural gas occurrence in the Joban Coal Field, Geological

* written in Japanese, with abstract in English.

Survey Spec. Pap. no. 210.

- HOSHINO, K. (1965b)*: Systematic fractures and fracture system in the sedimentary rocks and its application to disaster prevention, Paper of 2nd Symposium on Disaster Prevention.
- HOSHINO, K. (1966)*: Rock deformation and geologic structure, *Jour. Geol. Soc. Japan*, vol. 72, p. 105-116.
- INOUE, E. (1964)*: Paleogene system in western Nishisonogi Peninsula and sedimentary environment of lower Nishisonogi group, *Bull. Geol. Surv. Japan*, vol. 15, p. 166-188.
- JAEGER, J. C. (1964): Elasticity, fracture and flow, 2nd ed., John Wiley and Sons, Inc.
- KELLEY, V. C. & CLINTON, N. J. (1960): Fracture systems and tectonic elements of the Colorado Plateau, *Univ. New Mexico Pub. in Geology*, no. 6.
- KIMURA, T. (1966): Tectonic movements in the southern Fossa Magna, central Japan, analyzed by the minor structures in its southwestern area, *Jap. Jour. Geol. Geography*, vol. 37, p. 63-85.
- KITAMURA, N. (1962): Preliminary report on systematic jointing in the Taishu Group developed in Mitsushima-cho, Tsushima Island, Japan, *Sci. Rep. Tohoku Univ., Second Series (Geology)*, Spec. vol., no. 5.
- MOGI, K. (1964): Deformation and fracture of rocks under confining pressure (1), compression tests on dry sample, *Bull. Earthq. Res. Inst.*, vol. 43, p. 491-514.
- MOGI, K. (1965): Deformation and fracture of rocks under confining pressure (2), elasticity and plasticity of some rocks, *Bull. Earthq. Res. Inst.*, vol. 43, p. 349-379.
- MUELBERGER, W. R. (1961): Conjugate joint sets of small dihedral angle, *Jour. Geol.*, vol. 69, p. 211-219.
- MURAI, I. (1952)*: On fracture system developed in Neogene Tertiary rocks in the Bōsō Peninsula, *Jour. Geol. Soc. Japan*, vol. 56, p. 284.
- MURAI, I. (1955)*: Tectonic analysis of the district surrounding Fukui Plain, *Bull. Earthq. Res. Inst.*, vol. 33, p. 121-151.
- MURAI, I. (1965a)*: Fracture systems developed on the Island, Awa-shima, near the Epicenter of the Niigata Earthquake in 1964, *Bull. Earthq. Res. Inst.*, vol. 43, p. 611-624.
- MURAI, I. (1965b)*: The fracture system developed in the vicinity of Katsuura, the Bōsō Peninsula, *Bull. Earthq. Res. Inst.*, vol. 43, p. 829-869.
- NADAI, A. L. (1950): Theory of flow and fracture of solids, 2nd Ed., McGraw-Hill.
- NAGAHAMA, H. & MATSUI, K. (1958)*: 1 to 50,000 geological map with explanation "Kaki-no-Ura". *Geol. Surv. Japan*.
- NAGAHAMA, H. (1962)*: Yobikonoseto faulting in the Sakito-Matsushima coal field, Nagasaki Prefecture, Kyushu, Japan, *Jour. Geol. Soc. Japan*, vol. 68, p. 199-208.
- NIELSEN, R. P. & HOUGH, V. D. (1958): Regional orientation of joints in the Appalachian Plateau of Pennsylvania, *Geol. Soc. Am. Bull.* vol. 69, p. 1624.
- PARKER, J. M., III, (1942): Regional systematic jointing in slightly deformed sedimentary rocks, *Bull. Geol. Soc. Am.*, vol. 53, p. 381-408.
- PATTERSON, M. S. (1958): Experimental information and faulting in Wombeyan marble, *Bull. Geol. Soc. Am.*, vol. 69, p. 465-476.
- PRICE, N. J. (1959): Mechanics of joint in rocks, *Geol. Mag.*, vol. 96, p. 149-167.
- SANFORD, A. L. (1959): Analytical and experimental study of simple geologic structures, *Geol. Soc. Am. Bull.*, vol. 70, p. 19-51.
- SAKAKURA, K. (1964)*: Coal geology, *Gijutsu-shōin*.
- SHELDON, P. G. (1912): Some observations and experiments on joint planes, *Jour. Geol.*, vol. 2, p. 53-79; p. 164-183.
- SPENCER, E. W. (1959): Geologic evolution of the Beartooth Mountains, Montana and Wyoming, *Bull. Geol. Soc. Am.*, vol. 70, p. 467-508.
- SECOR, D. T. (1964): Role of fluid pressure in jointing, *Jour. Geol.*
- VER. STEEG, K. (1942): Jointing in the coal beds of Ohio, *Econ. Geology*, vol. 37, p. 503-509.
- WAGER, L. R. (1931): Jointing in the Great Scar limestone of Craven and its relation to the tectonic of the area, *Quat. Jour. Geol. soc. London*, vol. 87, p. 392-424.
- WISE, D. U. (1964): Microjointing in basement, Middle Rocky Mountains of Montana and Wyoming, *Geol. Soc. Am. Bull.* vol. 75, p. 287-306.

長崎県大島炭田地域の割れ目系

——特に節理の生成機構について——

星野 一 男

要 旨

節理は一般に面に沿う変位のない割れ目として定義されているが、堆積岩中の節理はしばしば密度の高い平行な割れ目群としてあらわれ、相当広い範囲にわたって規則的な分布を示すことが多い。このような systematic joints の成因についていろいろな説明が与えられてきたが、いわゆる extension fracture であつて汎地球的な営力により作られたとする考えと、地域的な造構応力により作られるもので断層と基本的に変わらないとする考え方とに最近まとめられつつある。野外調査では後者の考え方を支持するような結果が多いが、この場合、なぜ断層と同様に変位を伴わないのかという点が説明されねばならない。

大島は佐世保沖の小さな島で海岸線は凹凸に富み、干満の差も大きいため、干潮時にはひろい地域にわたって fracture pattern を連続的に追跡することができる。野外調査の結果方向、変位の性格、時代を基礎に A, B, C, D の 4 割れ目群が識別された。A 群は寺島によく発達する南北性の割れ目であり、A₂, A₃ 群は西彼杵層群後におこつた呼子瀬戸断層運動に関連してほぼ層理面に直交する最大主応力により作られたものと考えられる。B 群は東西性でこの地域で最も顕著に発達する割れ目群である。C 群はつねに層理面に直交しており C-1 群は走向に平行、C-2 群は走向に直交関係にある。D 群はきわめて小さな低角度の逆断層で走向・傾斜とも不規則である。

これらの割れ目群のうちで、B-1 群は最も普遍的、規則的な分布を示す典型的な節理を含んでいる。B-1 群は多くの場所で節理であるがほぼ 1 km の間隔で断層化されている。

B-1 a, B-1 b 群はそれぞれ左廻り、右廻りの変位を示し conjugate set をなしている。交差点には extension joints である B-1 c 群があらわれることが多い。B-1 群が最も顕著に発達する松島・西彼杵層群は 600 m の層厚を持つ砂岩・頁岩の累層で西に 10° 以内の低角度で単調に傾斜する非常におだやかな構造をなしている。松島・西彼杵層群の岩石が非常に brittle であること、堆積深度が浅いこと、おだやかな構造をなしていることは従来 systematic joints が作られやすいといわれている地質環境と一致している。

さらに節理が生成された応力条件を求めめるために 98カ所で求められた B-1 群の主応力線型から、割れ目が弾性変形、brittle 破壊をしたとの仮定のもとに Airy 函数と Mohr の破壊条件式を使つて B-1 群生成時の境界応力の大きさを計算した。その結果ほぼ南北方向の応力は引張りの応力 (tensile stress) である可能性が強いことが判つた。一方 B-1 群と密接な関係を示す B-2 群は層理面に直交する最大主応力により作られたことが明瞭であり、この地域ではほぼ B-1 群時から徐々に上昇応力が働き、それによつて南北性の tensile stress が発生し、この結果 B-1 群が作られたものと考えられる。

このような tensile stress のもとで破壊がおこるときには岩石は brittle な変形をおこしやすくきわめて小さな歪で割れ目を作るので無変位に近い割れ目がひろい範囲に発達する可能性が高いことが考えられる。

一般に従来節理と呼ばれていた割れ目は地層がこのような低い応力場で破壊されるときに、brittle な岩石中に生成される無変位の割れ目であるということができよう。

Kluftsystern der Insel Oshima, Kyushu; Eine Untersuchung ber Spaltung der spröden sedimentären Gesteine, mit spezieller Berücksichtigung von der Genese der Spaltung.

Zusammenfassung

Wegen der langen Strandlinie mit komplizierten, topographischen Zuständen, ist die Kleininsel. Ōshima, in nordwestlichen Kyushu bietet ein bestes Untersuchungsfeld zur Auffassung von ganzen kluftsystern der Insel an. Auf Grund von der Parallelität des Spaltenstreichens, der Verschiebungseigenschaft und der geologischen Bewegungszeit, sind vier Kluftsystern von sich unterschieden. Kluftsystern A hat drei Spaltgruppen, die alle beinahe N-S Streichen haben. System B besteht aus zwei E-N streichenden Gruppen. System A ist in der Ortschaft Terashima am merkwürdigsten verteilt, aber system B ist hervorragend in Ōshima und Ōtawā. System C ist die Klüfte, die zu den Schichtflächen senkrecht stehen, aber sie laufen parallel entweder zu Streichlinie oder zu Einfallrichtung. System D ist kleine inverse Verschiebungen mit wenigen obliquen Winkel, die die verschiedenen Streichen und Falten besitzen. In der Tabelle 6 stehen der Zustand des Vorkommens und Eigentümlichkeit von den hier gezeigten Kluftsystern.

Unter diesen Kluftsystern kommt allgemein die Gruppe B-1 am häufigsten vor, und stellt die regelmässigsten Spaltgruppe vor. Subgruppe B-1a and B-1b sind konjugierte Seitenverschiebungen, und der erstere ist sinistral und der letztere dextral. Die Gruppe B-1 stellt am besten in den Gebieten von Matsushima Formationsgruppe und Nishisonogi Formationsgruppe vor, die beiden aus den etwa 1,000 m mächtigen Sandsteinen und Tonschiefern bestehen. Sie fallen monoklinal nach West mit sanfter Neigung weniger als 10 ein. Die Gesteine sind fest und spröde unter dem 1,000 bis zu 1,500 bars hydrostatischen Druck.

An mehreren Orten zeigen die Spalten B-1 eine gute Parallelität, jedoch kommen sie als Verwerfung auf jeden ungefähr ein kilometer Abstand vor. Sehr selten ist aber die Aufschlüsse, wo die beiden Subgruppen B-1a und B-1b voneinander zusammen kreuzen. In den vermutlichen Kreuzungsstellen von beiden sind oft die Tensionbrüche, B-1e erschienen.

Bei 98 Stellen wurden die Hauptspannungen von B-1 festgestellt (siehe Fig. 11.). Maximale Hauptspannungslinie wird als eine etwas einfache Konkav-Kurve gegen Sud betrachtet. Wie das Medell der Fig. 32 zeigt, wurden die Grenzspannungen von diesen Kurven mit Hilfe der Airy-Funktion gerechnet, angenommen dass das Gestein spröde Deformation zeigte und unter Mohr's Bedingungen zerbrach. Das Berechnungsergebnis zeigt, dass Grenzspannungen entlang der minimalen Hauptspannungen mit etwa N-S Richtungen eine tensile Spannung sind. Geologische Auslegung deutet auch an, dass die Kluftsystern B, gleich wie System A, von den Hebungsbewegungen ausgebildet wurde, die entlang der Yobuko-Meeresstrasse Verwerfung mindestens zweimal nach der Nishisonogi Formationsgruppe bewirkt waren.

Es ist schlusslich zusammengefasst, dass die Spaltung die kluft mit keiner Verschiebung am der Kluftebene ist, die sich in den spröden Gesteinen unter niedriger Spannungsbedingungen wie tensiler Spannung ergibt.

PLATES
AND
EXPLANATIONS

(with 6 Plates)



Fig. 1 A part of Oshima Island: view of Hamaguri from the north.



Fig. 2 The Yobuko Strait from the north. Right side, Oshima. Left side, Terashima.



Fig. 3 The joints of B-la group in Yuridake formation in Hamaguri. They are the fractures crossing the picture, horizontally and accompanied by the fracture perpendicular to it.

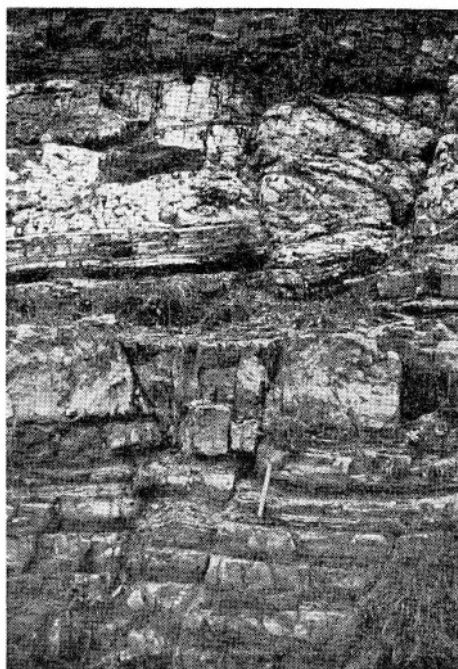


Fig. 4 The minor faults of B-la group by a road cut in Loc. 424, Ōta o, western Oshima.

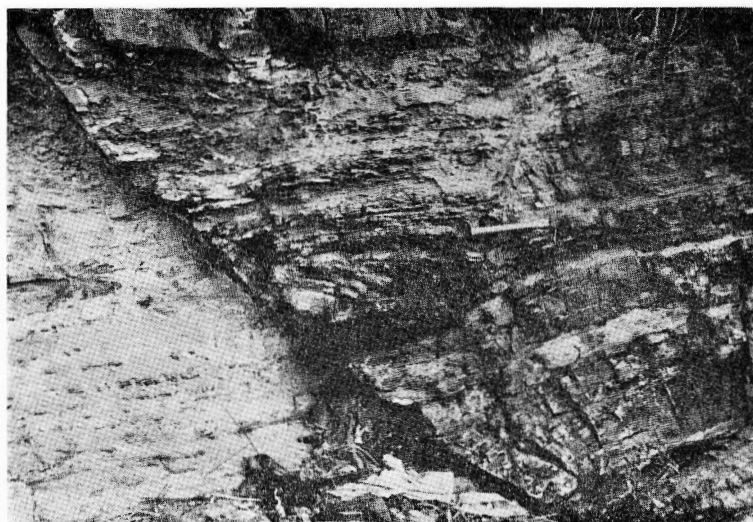


Fig. 5 A conjugate set composed of the faults of B-2 group, Loc. 256, Mase. This picture shows a part in the middle of Fig. 25.



Fig. 6 A group in Loc. 836, Terashima. See Fig. 15A.

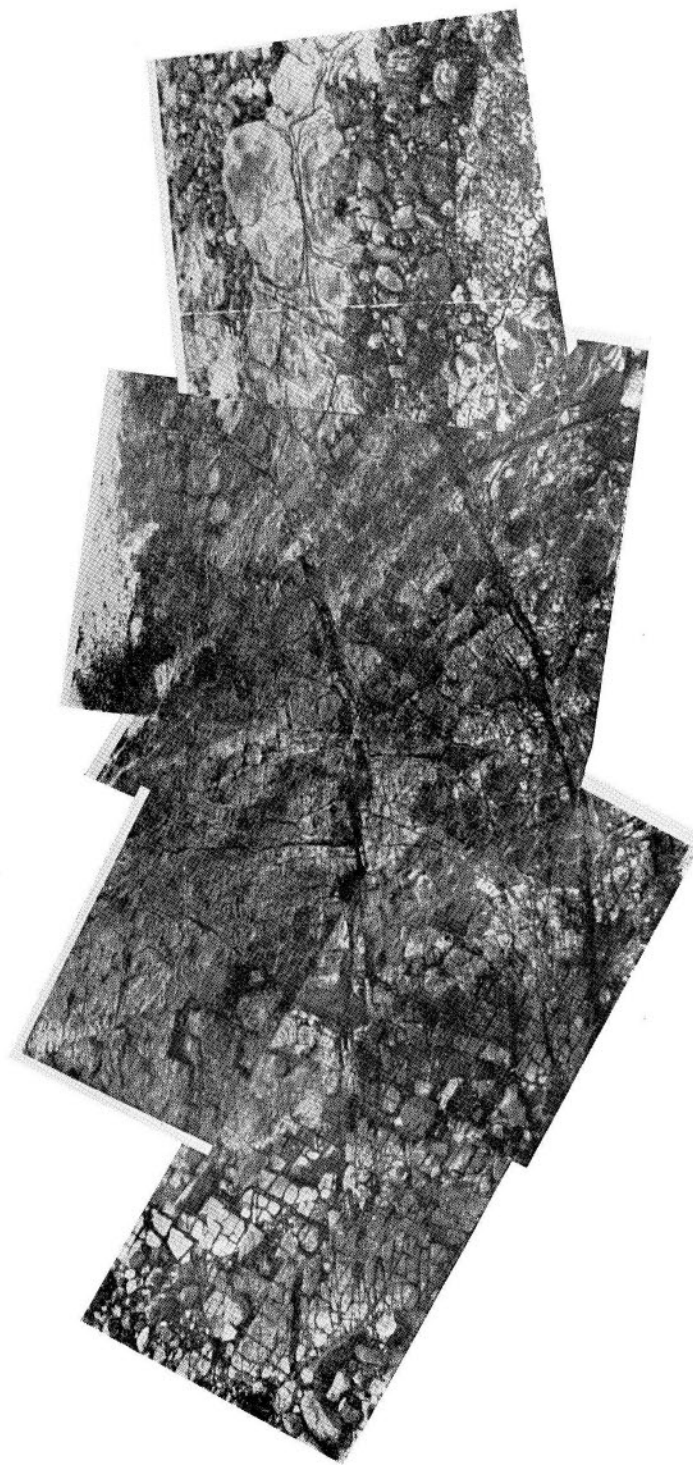


Fig. 7 Occurrence of B-lc. It occurs as if it connects B-la (left) with B-lb (right).
A hammer in left upper is a scale indicator. Near Oshima-machi.



Fig. 8 B-la set ; running from left upper to right below.
B-lb ; from right upper to left below.
B-lc ; running horizontally.

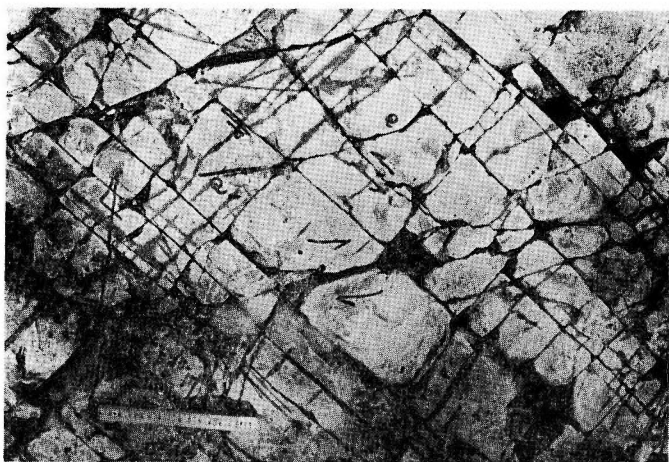


Fig. 9 Mode of displacement of B-1 set in Loc. 525, Shioda,
northwestern Ōshima.



Fig. 10 A. B-2 group grows out of B-1 sets, vertical view.
Loc. 21, Nakado.

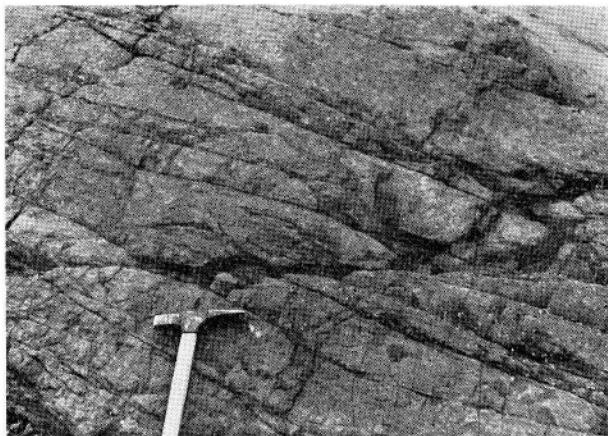


Fig. 10 B. B-2 group grows out of B-1 sets, horizontal view. See Fig. 24.



Fig. 10 C. B-1a intersects C-1 and C-2 sets. See Fig. 24.

地質調査所報告は1報文について報告1冊を原則とし、その分類の便宜のために、次のようにアルファベットによる略号をつける。

- A. 地質およびその基礎科学に関するもの
 - a. 地質
 - b. 岩石・鉱物
 - c. 古生物
 - d. 火山・温泉
 - e. 地球物理
 - f. 地球化学
- B. 応用地質に関するもの
 - a. 鉱床
 - b. 石炭
 - c. 石油・天然ガス
 - d. 地下水
 - e. 農林地質・土木地質
 - f. 物理探鉱・化学探鉱および試錐
- C. その他
- D. 事業報告

As a general rule, each issue of the Report, Geological Survey of Japan will have one number, and for convenience's sake, the following classification according to the field of interest will be indicated on each Report.

- A. Geological & allied sciences
 - a. Geology
 - b. Petrology and Mineralogy
 - c. Paleontology
 - d. Volcanology and Hot spring
 - e. Geophysics
 - f. Geochemistry
- B. Applied geology
 - a. Ore deposits
 - b. Coal
 - c. Petroleum and Natural gas
 - d. Underground water
 - e. Agricultural geology and Engineering geology
 - f. Physical prospecting, Chemical prospecting & Boring
- C. Miscellaneous
- D. Annual Report of Progress

地質調査所報告

第 217 号

KURASAWA, H.: Petrology of the Kita-matsuura basalts in the Northwest Kyushu, Southwest Japan, 1967

第 218 号

ISHIHARA, S.: Molybdenum mineralization at Questa Mine, New Mexico, U. S. A., 1967

第 219 号

高橋 稠: 地下水地域調査にみられる水温の総括的研究, 1967

第 220 号

斎藤正雄: 北海道の鉄資源, 1967

第 221 号

BAMBA, T. & SAWA, T.: Spilite and associated manganiferous hematite deposits of the Tokoro district, Hokkaido, Japan, 1967

REPORT, GEOLOGICAL SURVEY OF JAPAN

No. 217

KURASAWA, H.: Petrology of the Kita-matsuura basalts in the Northwest Kyushu, Southwest Japan, 1967 (in English)

No. 218

ISHIHARA, S.: Molybdenum mineralization at Questa Mine, New Mexico, U. S. A., 1967 (in English)

No. 219

TAKAHASHI, S.: On the ground-water temperature in Japan, 1967 (in Japanese with English abstract)

No. 220

SAITO, M.: On the iron resources of Hokkaido, Japan, 1967 (in Japanese with English abstract)

No. 221

BAMBA, T. & SAWA, T.: Spilite and associated manganiferous hematite deposits of the Tokoro district, Hokkaido, Japan, 1967 (in English)

Hoshino, K.

**Fracture System of Oshima Island, Kyūshū ; A Study of Jointing
in Brittle Sedimentary Rocks.**

Kazuo, Hoshino

地質調査所報告, No. 222, p, 1~56, 1967

41 illus., 6 pl., 6 tab.

Ōshima and its neighbourhood are composed of Eocene and Oligocene brittle sedimentary rocks, exhibiting less than 10 degree dipped isoclinal structure. Joint systems B-1 group and other prevail to be systematic over a whole area, and in some places the joints are faulted. Geological and mathematical analysis indicates that joints is the fracture with little displacement along the planes that would be formed in brittle rocks when the rocks fail in low stress field such as tensile stress.

551.24 : 553.94 (522.2)



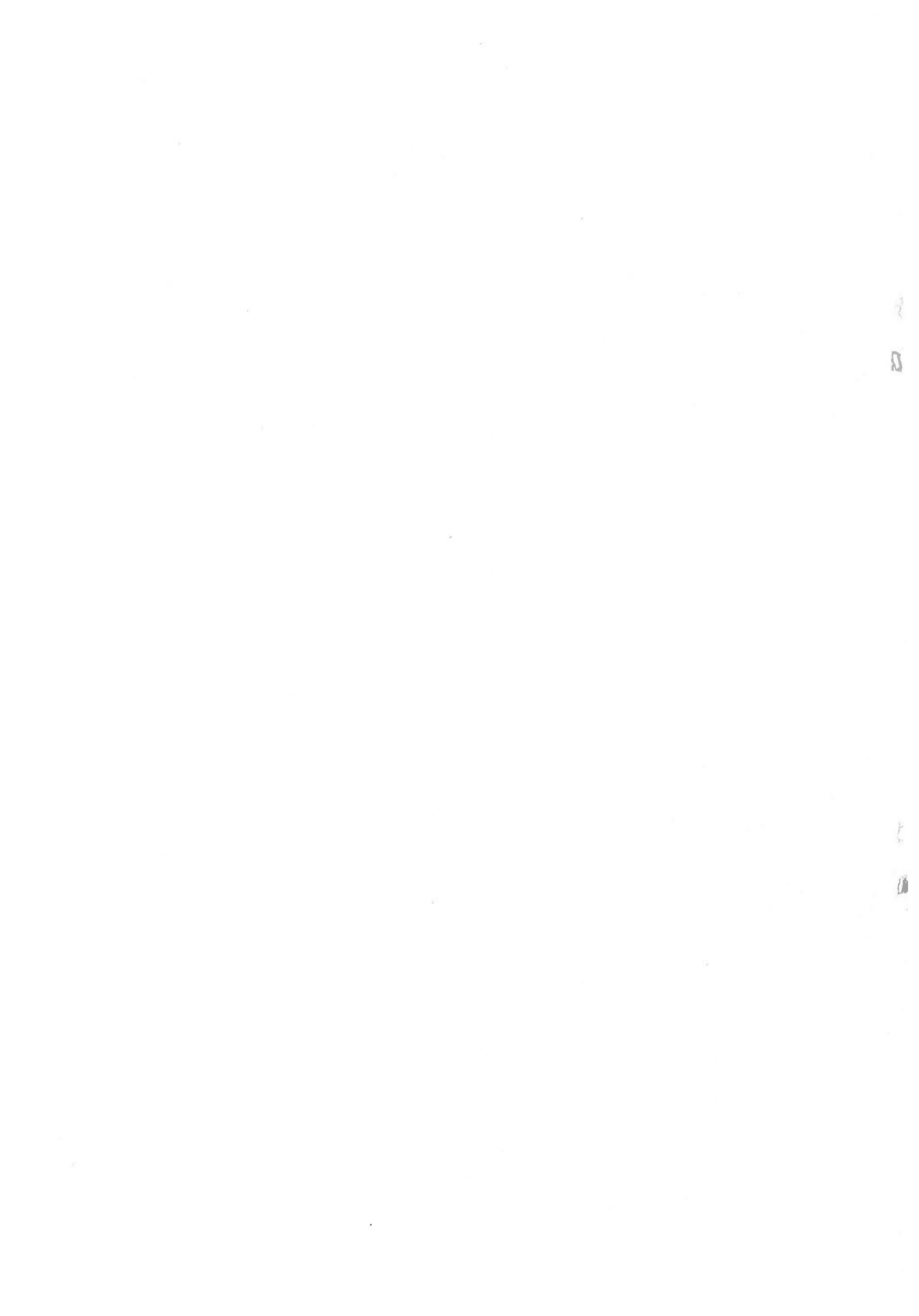
昭和 42 年 11 月 22 日 印刷

昭和 42 年 11 月 28 日 発行

工業技術院地質調査所

印刷者 坂 根 謙 吉

印刷所 株式会社坂根商店



地質調報
Rept. Geol. Surv. J.
No. 222, 1967